FINAL MASTER PROJECT

Master: *Nanostructured Materials for Nanotechnological Applications*

THE USE OF FUNCTIONALIZATION APPLIED TO NANOBIOTECHNOLOGY: Targeting cancer stem cells and regioselective functionalization of phages

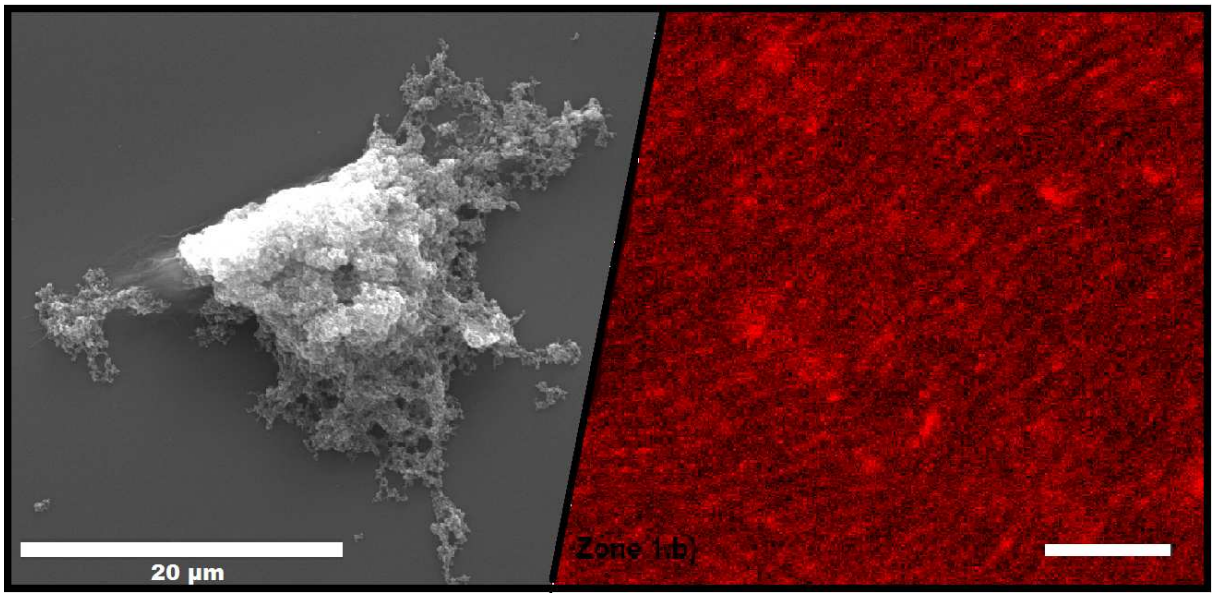

Carlos Piñol Domingo

FINAL MASTER PROJECT

Master: *Nanostructured Materials for Nanotechnological Applications*

THE USE OF FUNCTIONALIZATION APPLIED TO NANOBIOTECHNOLOGY: Targeting cancer stem cells and regioselective functionalization of phages

■ STUDENT:

▪ **Carlos Piñol Domingo**

■ CERTIFY:

♦ DIRECTOR:

▪ **Dr. Gerardo F. Goya Rossetti**_Condensed Matter Physics department (INA), Spain.

♦ CO-DIRECTORS:

▪ **Dr. María Carmen Visus Miguel**_Patology department, (Hillman Cancer Center-UPCI), Pittsburgh, USA.

▪ **Dr. Eric Grelet**_Self-Organization of Liquid crystals department (CRPP-CNRS), Bordeaux, France.

Science Faculty / University of Zaragoza
2012

INDEX

► GENERAL ABSTRACT

This work, composed of two subprojects, has been developed within the framework of two independent research lines on the functionalization and application of nanoprobes to nanobiotechnology field, specifically in biomedicine or biotechnology. The multidisciplinary research proposal involves physicists, chemists, biochemists and medical doctors, and therefore a part of the student's training work was performed at several centers abroad: The *Hillman Cancer Center* (UPCI), Pittsburgh, USA; the *Centre de Recherche Paul Pascal* (CRPP), Bordeaux and the *Institut National de la Recherche Agronomique* (BFP-IBVM), Villenave d'Ornon, France.

Example 1. The Cancer Stem Cell (CSCs) concept says that only a small proportion of cells within the tumor have tumorigenic capacity. These cells are usually chemo and radio resistance that is why it is believed that are responsible for tumor relapse and recurrence of cancer patients. There is an urgent need to develop cancer therapies that are effective in killing these specific tumor cells. Magnetic nanoparticles (MNPs), functionalized with specific monoclonal antibodies, can be generated to recognize CSCs target molecules within the tumors. Hyperthermia is a new approach of using these MNPs positioned in an alternating magnetic field (AMF) to produce localized heat and kill CSCs. Magnetic nanoparticles-induced hyperthermia is under investigation in different clinical trials on cancer patients. However, there is no information available on whether hyperthermia can eliminate CSCs. Therefore, the final goal of this project involve the application of hyperthermia to destroy CSCs and study the effect of this treatment in reducing tumor growth, increased cell death and improving the response to conventional therapies as chemo-radio therapy.

More particularly, this work has focused on the first steps of this strategy related to the preparation of antibody-functionalized MNPs (MNPs:anti-CDs) and their application to target CSCs for several tumor cell lines by fluorescence microscopy. It has also been supplemented with cytotoxicity studies by MTT assays and surface and intracellular distribution studies by scanning electron microscopy (SEM) technique.

Example 2. It is known that elongated viruses in concentrated solution self-organize into liquid-crystalline structures (mesophases) which exhibit different intermediate states between disordered liquids and perfectly organized crystals. Therefore, the introduction of specific functions by molecule grafting or nanoparticle bonding on the viral particles with a precise positional control, combined with the self-assembly properties of these functionalized

bioparticles, would give access to a wide range of applications in biosensing, memory devices, nanocircuits, light-harvesting systems, nanobatteries or MRI contrast agents. We used the mutant M13-C7C phage which presents a genetic mutation that allows the creation of unique binding sites on only one end of the filamentous virus through a pair of cysteine residues. The final goal of the project is to develop hybrid materials formed by the monitored assembly of these mutant M13-C7C phages with magnetic nanoparticles, with a 1:1 molar ratio, to induced highly sensitive nanorods by magnetic field, which are otherwise absent from the viral coat protein of the wild type phage.

More specifically, this work has focused in the mass production, amplification and purification processes, of the mutant M13-C7C phage which is during its growth in competition with the wild type one. We have then specifically studied the functionalization of these mutant phages with maleimide fluorophores, followed by the self-organization properties in order to validate our scientific approach.

• Keywords*: Nanobiotechnology; Nanofunctionalization; Cancer stem cells (CSCs); Magnetic nanoparticles (MNPs); Monoclonal antibodies; Viral nanoparticles (VNPs); Liquid crystalline structures.*

► RESUMEN GENERAL

Este trabajo, compuesto de dos subproyectos, se ha desarrollado en el marco de dos líneas de investigación independientes en la funcionalización y aplicación de nanosondas en el campo de la nanobiotecnología, específicamente en biomedicina o biotecnología. La propuesta de investigación multidisciplinar implica físicos, químicos, bioquímicos y médicos, y por lo tanto una parte del trabajo de formación del estudiante se realizó en varios centros en el extranjero: el *Hillman Cancer Center* (UPCI), Pittsburgh, USA; el *Centre de Recherche Paul Pascal* (CRPP), Bordeaux y el *Institut National de la Recherche Agronomique* (BFP-IBVM), Villenave d'Ornon, Francia.

Ejemplo 1. El concepto de célula Madre del Cáncer (CMC) dice que sólo una pequeña proporción de células dentro del tumor tienen capacidad tumorigénica. Estas células son normalmente quimio y radio resistentes, y es por lo que se cree que son responsables de la recaída y reaparición del tumor de pacientes con cáncer. Hay una necesidad urgente en desarrollar terapias contra el cáncer que sean efectivas en matar CMCs. Nanopartículas magnéticas (NPMs), funcionalizadas con anticuerpos monoclonales específicos, pueden ser generadas para reconocer moléculas diana de CMCs dentro de tumores. La Hipertermia Magnética (HTM) es un nuevo enfoque en utilizar las nanopartículas magnéticas (NPMs) posicionadas en un campo magnético alterno para producir calor localizado y matar las células tumorales. La hipertermia (HT) inducida mediante nanopartículas está bajo investigación en diferentes ensayos clínicos en pacientes con cáncer. Sin embargo no hay información disponible de sí la HT puede eliminar CMCs. Por lo tanto, el objetivo final de este proyecto implica la aplicación de la HT para destruir CMCs y estudiar el efecto de este tratamiento en reducir el crecimiento del tumor, aumentando la muerte celular y mejorando la respuesta a terapias convencionales como la quimio-radio terapia.

En concreto, este trabajo se ha centrado en los primeros pasos de esta estrategia, relacionadas con la preparación de NPMs funcionalizadas con anticuerpos específicos (NPMs:anti-CDs) y su aplicación en el marcaje de CMCs para varias lineas celulares tumorales mediante microscopía de fluorescencia. También se ha complementado con estudios de citotoxicidad mediante ensayos de MTT y estudios de la distribución intracelular mediante la técnica de microscopía electrónica de barrido (MEB).

Ejemplo 2. Es conocido que los virus elongados en soluciones concentradas se auto-organizan en estructuras de cristales líquidos las cuales exhiben diferentes estados

intermedios entre líquidos desordenados y cristales perfectamente organizados (mesofases). Por lo tanto, la introducción de funciones específicas mediante el injerto de moléculas o la adhesión de nanopartículas en las partículas virales con un control posicional preciso, combinadas con las propiedades de auto-ensamblado de estas biopartículas funcionalizadas, podría dar acceso a un amplio rango de aplicaciones en biosensores, dispositivos de memoria, nanocircuitos, sistemas acumuladores de luz, nanobaterías o agentes de contraste para MRI. Nosotros usamos el fago mutante M13-C7C el cual presenta una mutación genética que permite la creación de sitios de unión únicos exclusivamente en un extremo del fago, a través de un par de residuos de cisteína. El objetivo final del proyecto es desarrollar materiales híbridos formados por el ensamblado controlado de estos virus mutados M13-C7C con nanopartículas magnéticas (NPMs), con un relación molar 1:1, para inducir nanovarillas (nanorods) altamente sensibles mediante campos magnéticos, los cuales están por otra parte ausentes en la proteína de la cubierta viral de el fago de tipo silvestre.

Más concretamente, este trabajo se ha centrado en los procesos de producción en masa, amplificación y purificación, del fago mutado M13-C7C el cual está durante su crecimiento en competición con el tipo salvaje. Después hemos estudiado específicamente la funcionalización de estos fagos mutantes con fluoróforos de maleimida, seguido de las propiedades de auto-organización para tratar de validar un enfoque científico.

• Palabras clave: Nanobiotecnología; Nanofuncionalización; *Células madre del cáncer (CMCs); Nanopartículas magnéticas (NPMs); Anticuerpos monoclonales; Nanopartículas virales (NPVs); Estructuras cristalinas líquidas.*

I. GENERAL INTRODUCTION

1. Nanobiotechnology

Nanobiotechnology (*bionanotechnology* or *nanobiology*), a mix between nanotechnology and biotechnology, is extensively interdisciplinary because it combines physical principles, chemical properties, and biological characteristics. The great promise of nanobiotechnology stems from our burgeoning ability to design and synthesize self-assembling biostructures with better functionality, sensitivity, and specificity than synthetic organic or inorganic molecules **[1]**. This intersection of research fields is based on the perception that nanotechnology can offer biology new tools with a depth of understanding, while biological principles guide nanotechnology to new forms of highly complex functional nanosystems. Biological systems can guide the physical world of electronics, materials science, computation, and manufacturing in the assembly of complex functional devices and systems operating at the molecular and even atomic level *[see the FIG. 1]* **[2]**.

Nanomedicine is one of the fastest moving and most exciting research areas is the interface between nanotechnology, biology and medicine. This field presents many exciting possibilities for healthcare offering nanostructures as new therapeutic alternatives, which could revolutionize the areas of targeted/controlled drug delivery, disease detection, magnetic hyperthermia applied to cancer, biosensors or tissue engineering, and so on **[3]**. Another emerging and highly interdisciplinary field is *Viral Nanotechnology*, inhabiting the interface between virology, chemistry and materials science, in which viral nanoparticles (VNPs) are applied in diverse areas such as electronics, energy and next-generation medical devices **[4,5]**.

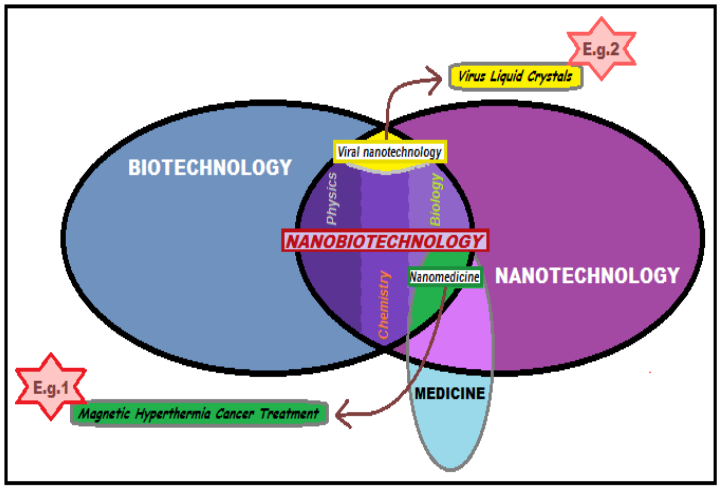

FIG 1. NANOBIOTECHNOLOGY. This is a mix of biotechnology and nanotechnology, which includes new fields such as viral nanotechnology (example 1) and nanomedicine (example 2).

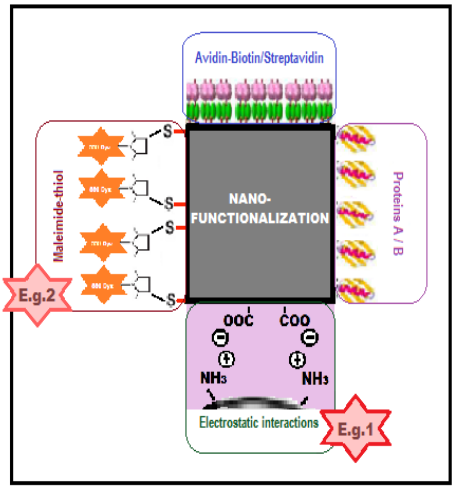

FIG 2. NANOFUNCTIONALIZATION PROCESS. Some examples are electostatic interactions, proteins A / G, biotin-avidin/Streptavidin and maleimide-thiol reaction.

2.- Nanoparticles and nanofunctionalization

Nanotechnology has brought a new generation of lightweight materials with superior mechanical and electrical properties **[6]**. An important example is the nanoparticle (NP), which is an excellent candidate for their further application in nanobiotechnology **[7]**. It is crucial to develop procedures for their adequate biofunctionalization, which ultimately confers the appropriate features for biotechnological and biomedical applications, such as specificity and bioactivity. Therefore, different strategies have been reported for their functionalization with relevant biomolecules such as *antibodies*, *viruses*, peptides, folic acid, vitamins, antibiotics DNA, carbohydrates, etc**. [8, 9]**.

The immobilization of biologically active molecules requires low density and good steric accessibility to active binding sites of the NPs **[10]**. Some examples of different immobilization protocols (nanofunctionalization process) are through non-covalent interactions, such as using exclusively electrostatic interactions (the most simple strategy), via immobilized protein A (presents high affinity to the Fc region of most ABs), through biotin-avidin/Streptavidin (the strongest known non-covalent biological interaction), or also by maleimide-thiol reaction (via covalent bonding assembly) *[see the FIG. 2]* **[11, 12, 13]**.

Two examples of the use of the functionalization applied to nanobiotechnology are reviewed in this report. In the first case, we will target cancer stem cells with antibody-functionalized magnetic nanoparticles for magnetic hyperthermia. The regioselective control of molecular nanoprobes on filamentous virus particles and self-assembly of these functionalized rod-like nanoparticles will be considered in the second case.

Bibliography

[1] H. Hess et al., Current Opinion in Biotechnology **21**, 373–375 (2010).

[2] R. Amin et al., NANO: Brief Reports and Reviews. 6:**2**, 101–111 (2011).

[3] T. D. Schladt et al., Dalton Trans. **40**, 6315–6343 (2011).

[4] J. Pokorski et al., Mol. Pharmaceutics. **8** (1**)**, 29–43 (2011).

[5] K. Koudelka et al., Current Opinion in Chemical Biology. **14**, 810–817 (2011).

[6] S. Bhaskar et al., Particle and Fibre Toxicology. 7:**3** (2010).

[7] C. Fang and M. Zhang et al., J Mater Chem. 1:**19**, 6258–6266 (2009).

[8] M. Moros et al., Nanoscale. **2**, 1746–1755 (2010).

[9] M.Arruebo et al., Cancers. **3**, 3279-3330 (2011).

[10] S. Puertas et al., J. Phys. D: Appl. Phys. **43** (47), 474012 (2010).

[11] P. Batalla et al., Process Biochemistry. **44**, 365–368 (2009).

[12] S. Puertas et al., Acs NANO. 5:**6**, 4521–4528 (2011).

[13] Avidin-Biotin Interactions: Methods and applications. Methods in molecular biology, Humana Press. **418** (2008).

II. EXAMPLE 1: Targeting cancer stem cells with antibody-functionalized magnetic nanoparticles for magnetic hyperthermia

1. INTRODUCTION

1.1. Cancer

Cancer remains as one of the most leading causes of death **[1].** Based on the *GLOBOCAN 2008 estimates* about 12.7 million cancer cases and 7.6 million cancer deaths occurred in 2008, accounting for 13% of all human deaths worldwide *[see the FIG. 1]*.

Cancer concept encompasses a broad group of diseases, all of them involving unregulated cell growth, in which cells divide and grow uncontrollably, forming malignant tumors and eventually have the potential to metastasize. Nowadays, the most common types of cancer treatments available are chemotherapy, surgery and radiotherapy **[2]**.

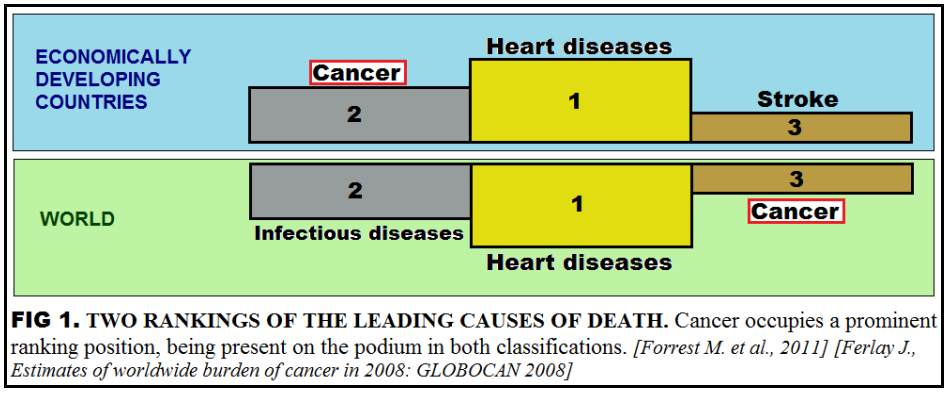

FIG 1. TWO RANKINGS OF THE LEADING CAUSES OF DEATH. Cancer occupies a prominent ranking position, being present on the podium in both classifications. *[Forrest M. et al., 2011] [Ferlay J., Estimates of worldwide burden of cancer in 2008: GLOBOCAN 2008]*

1.2. Cancer Stem Cells (CSCs): Concept, tumor cell lines and markers

What cells can be transformed to form tumors? To answer this central question in cancer biology was proposed the *stochastic model*. This theory believed for a long time hold that any tumor cell, uniform from a biological standpoint, can lead to new cancer *[see the FIG. 2, A) (left)]*. Unfortunately, this model seems to fail because the active programs responsible for the malignant process (tumor regeneration) are unlikely. Besides, experiments conducted during the last decades have shown that it is necessary up to a million human tumor cells or mouse to establish a tumor. Therefore, a new theory has recently emerged. This is the *hierarchical theory* that suggests that tumor cells are heterogeneous from a functional point of view and could be organized in a hierarchy where there are a minority population

within the tumor cell mass in each type of cancer, the ***CSCs***, constituting the bulk of the cancer cells within the tumor in most cases *[see the FIG. 2, A) (right)]*. These "tumor initiating cells" have characteristic properties both of normal stem cells, such as capacity of self-renew and the potential to divide asymmetrically generating any cell type within the tumor; and also of tumor cells, dividing uncontrollably (a large number of times) and leading the expansion of the tumor. Given its properties, it has been postulated that the CSCs may arise from mutations in normal stem cells, which are found in many tissues. In some cases, these CSCs may be very resistant reservoirs to radiotherapies and chemotherapies, being responsible for the relapse of a tumor (reappearance frequently observed in many cancers) or even give rise to metastases *[see the FIG. 2, B)]*. Therefore, since conventional therapies often increase the fraction of tumorigenic cells in cancer, the experimental results suggest that only those treatments capable of eliminating the CSCs may prevent an effective and lasting recurrence **[3-6].**

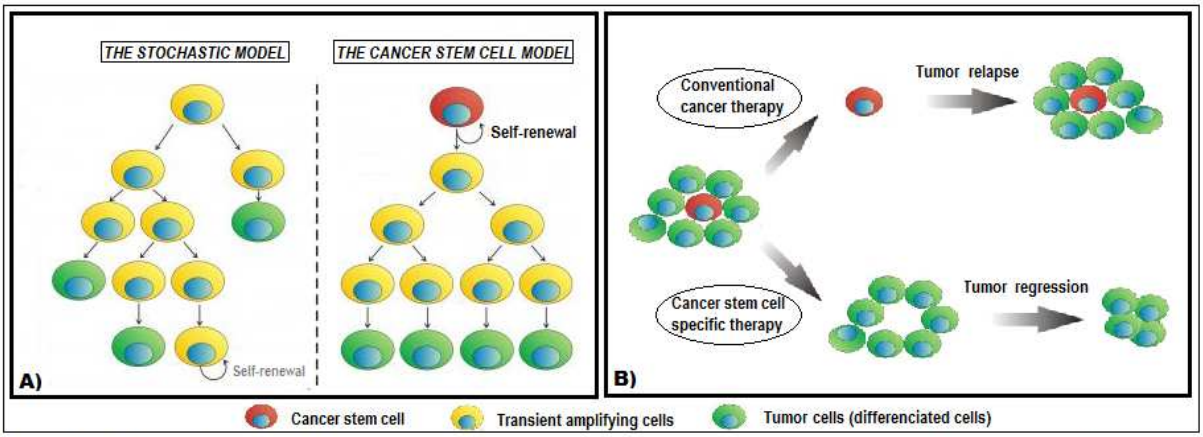

FIG 2. CANCER STEM CELLS (CSCs). A) Two important theories have been proposed to understand the biology of cancer. **B)** The CSC specific therapy was postulated to explain the relapse of tumors after the conventional cancer therapy. *The images were taken of the EuroStemCell webside.*

Recently, putative CSCs have been discovered in many different solid tumor types. Examples include the *Head and Neck Squamous Cell Carcinoma (SCCHN) cell line PCI-13*, an epithelial tumor with hardly any improvement in the treatment during the last 30 years, containing about < 10 % of CSCs within the tumor **[7 - 9]**. *Breast cancer cell line MDA-MB-231*, also an epithelial tumor where the CSCs, discovered in 2003, are representing only 2% of the total mass of breast tumor cells **[10, 11]**. The *human neuroblastoma cell line SH-SY5Y*, the most commonly diagnosed tumor in infants, with a population of CSCs appears to represent between 0.3% and 25.1% of the tumors examined **[9]**. Also, recently it has been discovered CSCs of the *pancreatic cancer cell line MIA PaCa-2*, a lethal epithelial tumor usually diagnosed in an advanced state **[12, 13]**.

How have the CSCs been identified? Thanks to a variety of markers expressed by the CSCs (*CSCs markers*) such as cell-surface proteins (CD133, CD44, CD34), cytoplasmic proteins (ABC transporters) and enzymes (Aldehyde dehydrogenase [ALDH1]) and so on. It must be taken into account that the vast majority of cells, which express these markers, are not stem cells and the markers considered from one organ are frequently not useful for identifying stem cells in other tissues **[6]**. The combination of these markers, for instance CD133 and CD44, two star markers, is believed that could be specific CSCs markers for many tumors **[4]**. On the one hand, ***CD133***, a glycosylated transmembrane cell surface antigen with unknown function so far, is restricted to stem cells since is considered an early (proliferative) antigen expressed on primitive progenitors (such as pancreatic islet cells or placenta) and some leukemias **[14-16]**. It has been found that this marker labels CSCs of brain (e.g. SH-SY5Y 2.7%), prostate, intestinal, pancreatic, ovarian, colorectal, lung and liver cancers **[17]**. On another hand, ***CD44***, a highly glycosylated type-I transmembrane cell surface receptor protein involved in cell/matrix interactions, is widely expressed on most cell types. This CSC marker is typically expressed in breast, colorectal, ovarian, liver, SCCHN or pancreatic cancers **[4, 14]**.

1.3. Magnetic nanoparticles (MNPs) as agents for hyperthermia

MNPs are submicron moieties with special magnetic properties, made of inorganic or organic materials, which may or may not be biodegradable **[18]**. MNPs for biomedical applications must be highly stable over time, unrecognizable by the immune system (with biocompatible polymers), have low levels of toxicity and a high magnetic moment which minimizes the required doses **[19]**. The iron-based NPs (mainly magnetite, Fe_3O_4) have provided today the best results in relation to its cytotoxicity and final biodistribution in the body **[1, 20, 21]**. A useful method in cytotoxicity studies, very simple, accurate, yields reproducible results, is the *MTT essay*, which consists of viable (living) cell determination spectrophotometrically as a function of mitochondrial activity in living cells. Compared to conventional therapies, nanoparticles (NPs) show several advantages in cancer treatment (or diagnosis) due to they can be synthesized in specific sizes (10-100 nm) and with surface characteristics to penetrate tumours. Besides, they can also be engineered to penetrate cells and physiological barriers or to target tumour cells (surface functionalization) with biomolecules by attaching to tumor-specific cell markers.

Magnetic Hyperthermia (MHT), one of the promising approaches in cancer therapy **[22]**, consists of heating the target tissue ($44 < T < 46$ º C), by remote application of an

alternating magnetic field applied on previously incorporated MNPs to CSCs. The purpose of this non-invasive and highly selective technique is to inhibit the proliferation of CSCs with the aim of destroying or rendering them more sensitive to the effects of conventional protocols of radiation and chemotherapy **[23, 24].** A significant improvement in clinical outcome with improved overall survival, as compared to patients who only receive radiotherapy or chemotherapy, has been demonstrated for tumors of the SCCHN, breast, brain, and so on **[25, 26]**. Certainly this technique depends on the efficiency to transport the MNPs into the CSCs (target cells) to be heated, so that a central part of this technique is to implement an effective strategy for vectorization of these NPs. A good choice is to use of the monoclonal antibodies (ABs or anti-CDs) (other options are carbohydrates, peptides or nucleic acids) to recognize different CSCs markers, thanks to their unique properties which there are sensitivity, selectivity and specificity **[27]** *[see the FIG. 3]*.

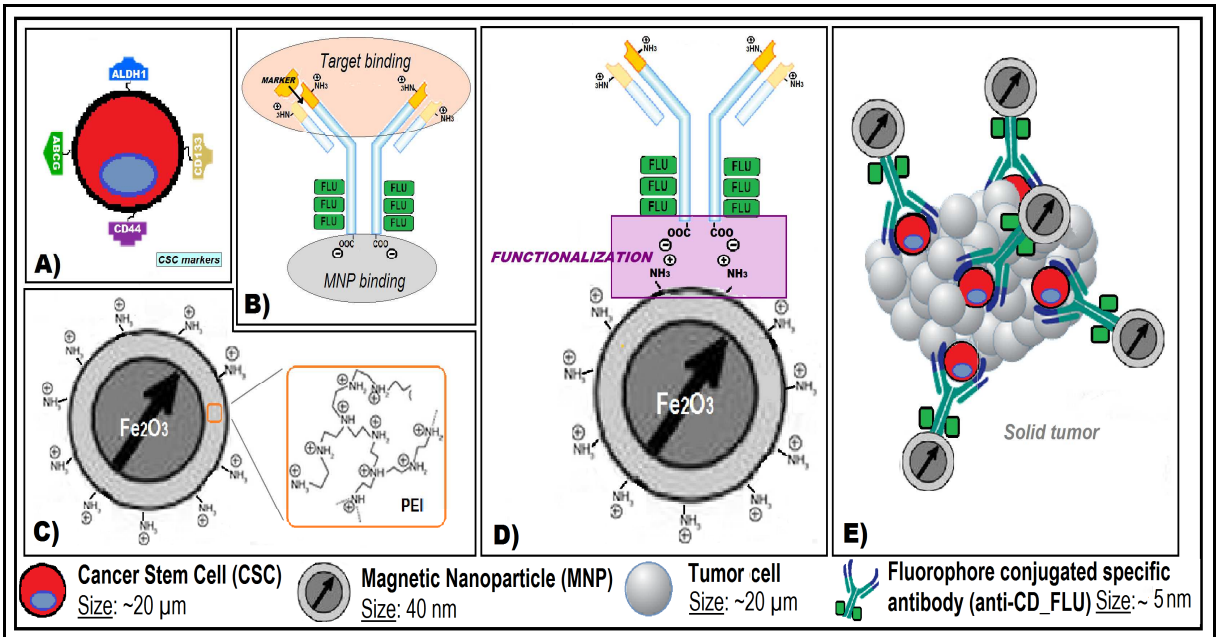

FIG 3. SCHEME OF THE PROPOSED STRATEGY: Preparation of the antibody-functionalized MNPs and their application to target CSCs for several solid tumor lines. **A)** Different markers expressed by the CSCs (CSCs markers). There could be one or several of these CSCs markers in every CSC, depending on the type of tumor cell line. **B)** Monoclonal antibody structure. All the antibodies (AB) used have an isoelectric point of ~7.3. Antibodies are divided in two diferent parts, the Fab region that corresponds to the target (markers) binding and the Fc region where the MNPs will be attached. Besides, This ABs are conjugated in the Fc region with about 6 molecules of fluorophore (FITC/PE) for each molecule of AB. **C)** Monodisperse MNPs of 25 kDa with a concentration of 3.44 mg/mL and a particle size of 40 nm, composed of a Fe3O4 core and polyethylenimine (PEI) shell, were used. The PEI shell creates a highly branched polymer with about 25% primary, 50% secondary and 25% tertiary amine groups. The isoelectric point (Zeta potential) is at around 9.2, therefore, positively charged for values below of pH. *These MNPs had been synthesized and characterized by Dr. Pilar Calatayud and Beatriz Sanz from the hyperthermia group of the Institute of Nanotechnology of Aragon (INA).* **D)** Functionalization process. This process will be carried out by electrostatic interactions, in a way that the Fab is free to interact with the CSC markers. **E)** CSCs targeting process with ABs-functionalized MNPs, shown for a solid tumor. This process corresponds to the last aim of this work.

2. AIMS

Several experiments designed to achieve the targeting of CSCs with MNPs, previously functionalized with anti-CDs, are reviewed in this work:

- **To determine the cytotoxicity of the Magnetic Nanoparticles (MNPs) on the tumor cell lines**. Cytotoxicity studies will be carried out for each line by MTT essays, modifying the concentration of nanoparticles (NPs) and the times of incubation.

- **To study the surface and intracellular distribution of the NPs treated-tumor cells**. It will carry out the incubation of the tumor cells lines with the MNPs, analyzing both the affinity between MNPs and tumor cells by Neubauer chamber counting and also the intracellular distribution of the cancer cells by Scanning Electron Microscopy (SEM).

- **To functionalize the MNPs with specific anti-CDs and CSCs targeting**. The synthesis of the fully functional MNPs with highly specific markers, anti-CD44 and anti-CD133, and the characterization of the resulting complex (MNPs-anti_ABs) in terms of stability and functionality, with the targeting of CSCs, will be studied by fluorescence microscopies.

3. EXPERIMENTAL SECTION

3.1. MATERIAL *[see the FIG. 3]*

▪ **Magnetic nanoparticles (MNPs)**. Monodisperse MNPs with a particle size of 40 nm, composed of a Fe_3O_4 core and PEI shell, were used.

▪ **Tumor cell lines**. Four tumor cell lines have been used throughout the life of this project. On the one hand, *SCCHN cell line PCI-13*, *breast cancer cell line MDA-MB-231* and *pancreatic cancer cell line MIA PaCa-2* were used during the stay in the Hillman Cancer Center. These cell lines were either established at the University of Pittsburgh Cancer Institute. On the other hand, *human neuroblastoma cell line SH-SY5Y*, a cell line established at the Institute of Nanoscience of Aragón (INA), was used during the stay in the INA.

▪ **Monoclonal antibodies (ABs or anti-CDs)**. It has worked with two monoclonal antibodies:

  ▫ CD44 (HI44a) – FITC Antibody, human. *[Clone: HI44a (isotype: mouse IgG2a), purchased from MACS Miltenyi Biotec]*. This CD44 antibody (anti-CD44), conjugated to

Fluorescein isothiocyanate (FITC), anti-CD44_FITC, recognizes an epitope of the CD44 antigen.

▫ CD133/1 (AC133) – PE antibody, human *[Clone AC133 (isotype: mouse IgG1), purchased from MACS Miltenyi Biotec]*. This CD133 antibody (anti-CD133), conjugated to R-phycoerythrin (PE), anti-CD133_PE, recognizes an epitope of the CD133 antigen.

3.2. PROTOCOLS

▫ Note*:* In the *APPENDIX 1* are shown some protocols when working with tumor cells.

3.2.1. MTT protocol for cytotoxicity studies.

DAY 1 – The tumor cells were seeded onto three 96-well plates (a plate for each essay time) at 10^6 cells mL^{-1} (10^5 cells per well). Each plate contained three-quarter parts of the wells with the three tumor lines, corresponding to a quarter for each one; and the last quarter of every plate without cells (only growth medium), used as a negative control.

DAY 2 – 100 μL of MNPs medium at different concentrations were added to each one of the wells. Seven different concentrations, for each line of the plate, ranged from 1 to 200 μg MNPs mL^{-1} medium (1, 2, 5, 10, 50, 100 and 200 μg MNPs mL^{-1} medium), and the last line without MNPs used as a negative control (prepared in triplicate). These samples were cultured overnight at 37ºC.

DAY 3, 4 and 5 – The following procedure was repeated with the pertinent plaque for each time. To perform the colorimetric test, 100 μL of medium of each well were removed gently, incubating the samples with 10 μL (5 mg mL^{-1}) MTT at 37ºC for 3h. The resultant formazan crystals were dissolved in 100 μL of lysis buffer. The absorbance was measured by a microplate reader (ELISA) at 550 nm. An important aspect to take in account is the removal of any bubbles to avoid interferences in the measurements.

3.2.2. Protocol for studying the affinity between MNPs and tumor cell lines.

DAY 1 – Three cell culture flasks for every tumor cell line containing 6.7 x 10^5 tumor cells each of them (1.34 x 10^5 cells mL^{-1}) were prepared. Subsequently, 15 μL of MNPs (10.32 μg mL^{-1}) were added into two of the three replicates. The last one was used like control. Then, all samples were incubated overnight at 37ºC.

DAY 2 – The harvesting and the counting of tumor cells lines were carried out, as are explained in the point *protocols for working with tumor cells* of the *APPENDIX 1*. Then, the samples were passed down a magnetic column (*OctoMACS^{TM} Separator, MACS Miltenyi Biotec*), obtaining the respective flow thru of each sample. Subsequently, the magnetic columns were disengaged from the separator and several PBS volumes were passed down through to obtain the eluates. Finally, it was carried out the counting of the tumor cells, of both flow thru and elutes, in the same way than the last time.

3.2.3. Protocol for TEM/EDX sample preparation.

DAY 1 – The SH-SY5Y cells were seeded onto a 24-well plate at 5 x 10^4 cells mL^{-1} (5 x 10^4 cells per well). A sterile cover slip had been added in each well used in the assay, previously. The tumor cells were cultured overnight at 37ºC.

DAY 2 – Cells were washed twice with PBS and the MNPs media, at different concentration, were added into wells each. The first well was used as a negative control and the following to the well 6 contained 1.25, 2.5, 5, 25 and 25 μg MNPs mL^{-1} medium (two replicas). The tumor cells with and without MNPs were cultured overnight at 37ºC.

DAY 3 – The growth medium of each well was removed, containing any cell that may have been peeled away and the MNPs that not have been incorporated or anchored into the tumoral cells. The samples were washed twice and afterwards fixed with 2.5% glutaraldehyde in 0.1M sodium cacodylate buffer with a 3% sucrosa solution for 90 min at 37ºC. After the fixation, the samples were re-washed twice and the dehydratation process was conducted by incubating the cells at RT with increasing concentrations of methanol, through following steps in duplicate: Firstly, MeOH 30%, 50%, 70% for 5 min each one; secondly MeOH 100% for 10 min; and finally, MeOH 100% anhydride for 5 min. The prepared samples were preserved into anhydride methanol in the refrigerator at 4-8ºC, waiting for the next step. Finally, all cover slips were sputter-coated with gold, remaining as intact samples until they were analyzed by SEM (*SEM INSPECT F50, FEI Company*) and EDX.

3.2.4. Protocols for the studies both the interaction between MNPs:anti_CDs and the targeting of CSCs with these antibody-functionalized MNPs.

Firstly, 10 μL of each anti-CD (or only one, depending of the sample) anti-CD44_FITC or/and anti-CD133_PE and different ranges of MNPs concentration were added into each eppendorf, containing 500 μL of TRIS buffer at pH:7.9. In addition, several

negative controls were also prepared, where the first one corresponded to the negative control with only buffer (without MNPs and anti-CDs), the second one only contained 10μL of each anti-CD and the last one contained exclusively MNPs. These samples were stirred by vortex and incubated for 1 hr at RT. Secondly, magnetic separation of the samples were carried out using a *Magnetopure size big (Chemicell)*. To this end, each eppendorf was inserted into the magnetized wells and steeping for 30 min. Finally, the supernatants were isolated and analyzed by spectrofluorometry on the one hand, and the pellets by fluorescence microscopy on the other.

3.2.4.1. Protocol for spectrofluorometer sample preparation.

The supernatants obtained were analyzed by spectrofluorometry, using a *LS5S luminescence spectrometer (Perkin Elmer Life Sciences)*. The intrinsic fluorescence spectrum was monitored from 496–600 nm upon excitation at 496 nm in 0.5 cm path length plastic disposable cuvettes. In advance, optimization process was carried out with the best slit width and preparation of the standard curves for both anti-CDs and MNPs, or without MNPs.

3.2.4.2. Protocol for sample preparation for fluorescence microscopy.

DAY 1 – SH-SY5Y cells were seeded onto a 24-well plate at 10^5 cells mL^{-1} (10^5 cells per well). A sterile cover slip had been added in each well used in the assay, previously. The tumor cells were cultured overnight at 37ºC.

DAY 2 – Cells were washed twice with PBS and the culture mediums containing the pellets related to the essay in basic media (TRIS buffer at pH=7.9) were added in each well. The first two wells were used as a negative control, where the first one corresponded to the negative control without MNPs or anti-CDs, and the second one was the negative control only with 10 μL of each anti-CD. These samples were cultured overnight at 37ºC.

DAY 3 – The growth medium of each well was removed, containing any cell that may have been peeled away and the conjugates that not have been incorporated or anchored into the tumoral cells. The samples were washed twice and afterwards fixed with 4 % PFA for 15 min at RT. After the fixation, by helping with tweezers and outside the laminar-flow, the cover slips were washed three times sequentially submerging into different beakers with the following sequence of fluids: PBS, PBS, Milli-Q. Then, the treated cover slips were fixed on slides. To that end, 5 μL of Mowiol-DAPI solution was added on a slide for

every sample and dropped carefully the cover onto the solution, trying to avoid formation of air bubbles between slide and cover.

DAY 4 – Finally, each cover was fixed stronger on the cover slip with nail polish. The fluorescent samples must be kept in the dark to avoid any degradation.

4. RESULTS AND DISCUSSION

4.1. Cytotoxicity studies of the MNPs on the tumor cell lines by MTT essay

The cytotoxicity produced by MNPs is an important obstacle that needs to be overcome for biomedical applications. Therefore, it is fundamental to determine how the MNPs are affecting to the viability of any type of cell inside the bloodstream. In this project was delimited the study for several tumor cell lines. For that, MTT cell viability assays were carried out to analyze the toxicity caused by the MNPs in several tumor lines (Mia PaCa-2, PCI-13 and MDA-MB-231) at different times; in this case, every 24 hours for three days *(see the protocol in previous experimental section 3.2.1.)*.

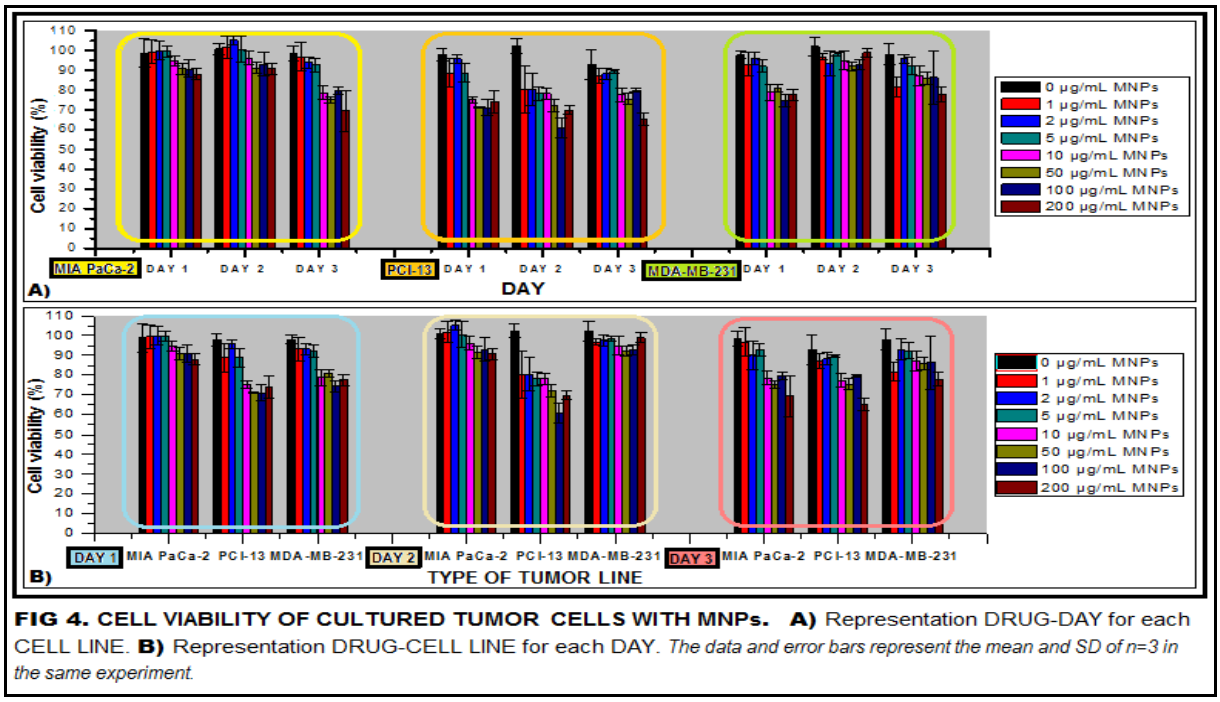

FIG 4. CELL VIABILITY OF CULTURED TUMOR CELLS WITH MNPs. **A)** Representation DRUG-DAY for each CELL LINE. **B)** Representation DRUG-CELL LINE for each DAY. *The data and error bars represent the mean and SD of n=3 in the same experiment.*

The results showed a decreasing trend for each cell viability bar, pertaining to each tumor cell line, when the MNPs concentration is increased from 10 µg mL^{-1} to 200 µg mL^{-1} [see the FIG. 4]. More specifically, *there was not observed a loss of viability to 5 µg mL^{-1}, and from here there were a proportionately reduction to the higher concentration studied, with a*

net loss of cell viability around the 20 percent. There seems not to exist an obvious loss of the viability of tumor cell lines over time, from day 1 to 3.

Furthermore, *these cancer cells seem to attach (or internalize, it is not clear) with the MNPs, as there seems shown in the fluorescence images taken during this cytotoxicity essay* (*see the photos in the Appendix 1*). It was also observed *the agglomeration of the MNPs, at high concentration, which is a problem to take into account.*

It should also be noted that if the results would have been positive, showing a toxic effect these MNPs for the tumour cell lines studied, the application of hyperthermia would not have been needed. Actually, it is fundamental to work with non-toxic MNPs because if they were capable to destroy very resistant cells, such as tumor cells, to kill the normal cells would be more very simple.

4.2. Study of the affinity between MNPs and tumor cell lines

In order to get an idea regarding the affinity between the MNPs and the tumor cell lines, whether or not take place their uptake, a simple essay of cell counting was carried out by Neubauer chamber counting *(explained in the experimental section 3.2.2.)* [*see the FIG. 5*].

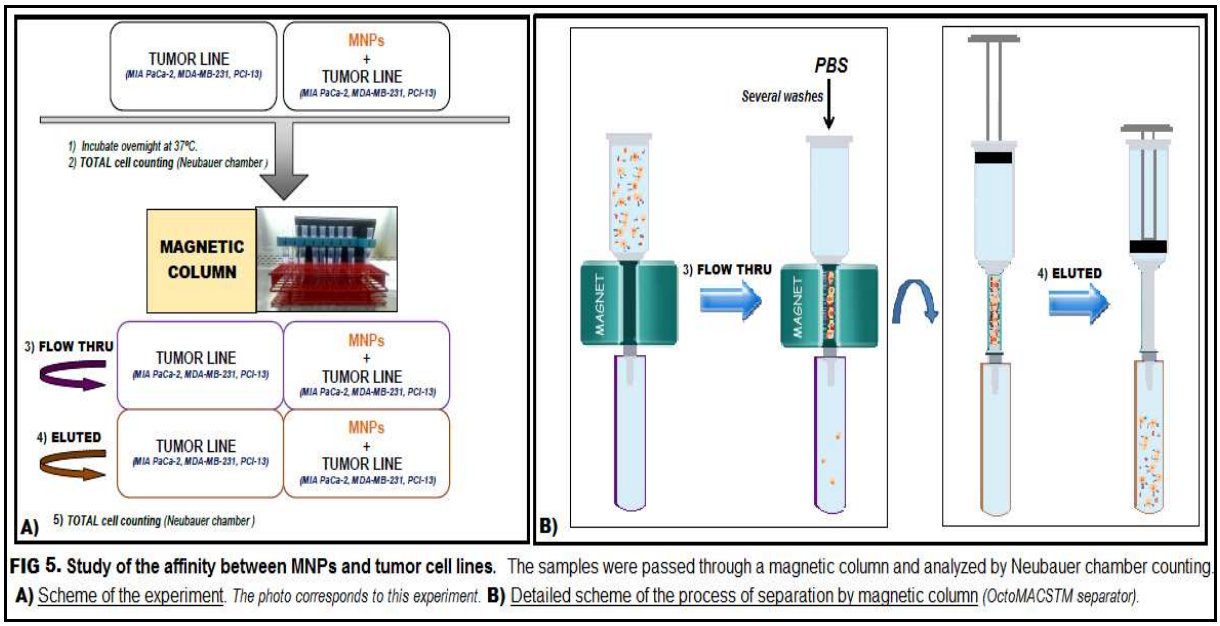

FIG 5. Study of the affinity between MNPs and tumor cell lines. The samples were passed through a magnetic column and analyzed by Neubauer chamber counting. **A)** Scheme of the experiment. *The photo corresponds to this experiment.* **B)** Detailed scheme of the process of separation by magnetic column *(OctoMACSTM separator).*

The results for every tumor cell line could be three replicas of the same essay because of the similarity. The flow-thru, which corresponds to the cells not attached on the magnetic column, only show positive results for the cells without MNPs. On the contrary,

exclusively the population of the cells with the MNPs has been obtained in the eluates, which correspond to the cells attached on the magnetic column. T*hanks to this experiment, it has been proved that practically all cells attach or internalize the MNPs for each tumor line studied (PCI-13, MIA PaCa-2 and MDA-MB-231).*

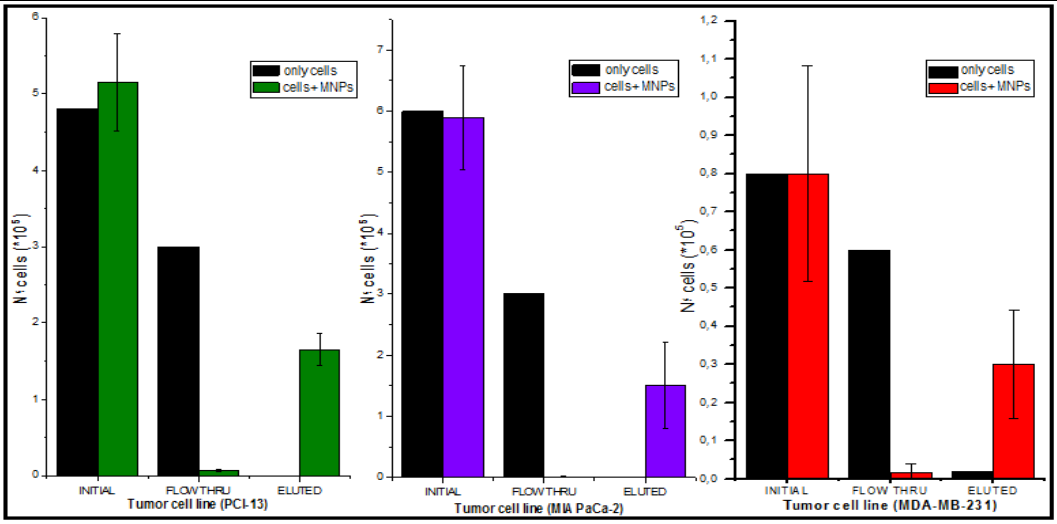

FIG 6. Study of the affinity between MNPs and tumor cells. Representation of Nº CELLS for each CELL LINE. The samples has been analyzed by Neubauer Chamber Cell Counting. *The data and error bars represent the mean and SD of n=2 in the same experiment.*

4.3. Study of the surface and intracellular distribution of the MNPs treated-tumor cells by TEM/EDX techniques

We have already demonstrated that tumor cells interact with the MNPs, but it doesn't know if there exists the internalization of them. Subsequently, a much more comprehensive study was carried out using two more powerful techniques such as Scanning Electron Microscopy (SEM), which provides high-resolution and long-depth-of-field images of the sample surface, and Energy Dispersive X-ray Spectroscopy (EDX), offering elemental identification of almost any element of the periodic table *(explained in the experimental section 3.2.3.).*

Clear differences in the tumor cell surface were observed between the cultured tumor cells with and without MNPs *[see the FIG. 7]*. The blank sample, belonging to the control without MNPs, showed the normal morphology of these kind of cells, which is a large extension of the axon (that conducts electrical impulses away from the neuron's cell body), and the long and branched projections of the dendrites (that act to conduct the electrochemical stimulation received from other neural cells to the cell body). In contrast, in the case of the tumor cells cultured with MNPs, it was observed a reduced cell extension with much more

delimited cell morphology due to the presence of short dendrites even further branched. Furthermore, unlike the control, these samples exhibited a cell membrane filled with roughness. These membrane deformations seem to show that the tumor cells contain material inside, therefore, *it is likely that the MNPs were also internalized apart from carried out the MNPs adhesion on the surface.* These observations present the same trend with increasing concentration of MNPs from 5 to 25 μg mL^{-1}.

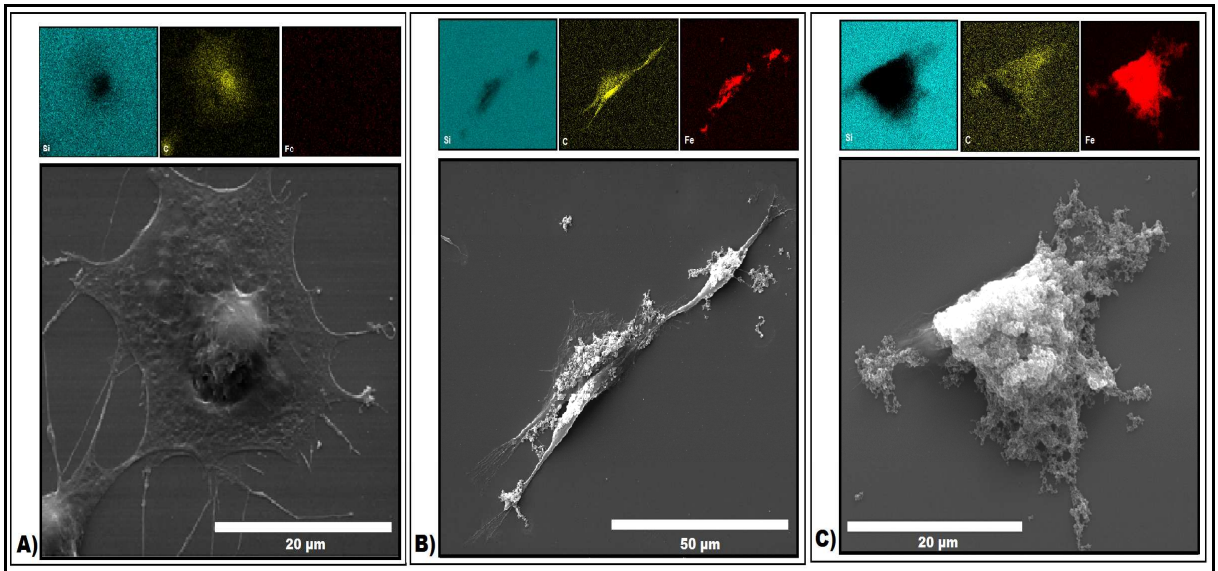

FIG 7. Study of the surface and intracellular distribution of the MNPs treated-tumor cells by TEM and EDX. A magnified image of the SH-SY5Y tumor cells taken by SEM and three photos of the same picture taken by EDX, which analize the presence of Si, C and Fe respectively for each sample, are shown in every case. **A)** BLANK (only cells); **B)** 5 mg/mL of MNPs; **C)** 25 mg/mL of MNPs. *SEM images were taken at 5 and 30 kV with a FEG column by the SEM INSPECT F50 (FEI company). The photos and the analysis of data were realized by Carlos Cuestas Ayllón and Teobaldo Torres Molina in the INA.*

Thanks to the second technique used, EDX, it was definitely corroborated that we have effectively iron material in the samples, corresponding to the MNPs. Clearly, it is observed an expanding red spot on the tumor cells with increasing concentration of MNPs *[see the FIG. 7]*. These figures give us also information about the distribution of the carbon (integral element of living systems) or the silice (the SiO2 is the major component of cover slip) in each sample.

These samples were also analyzed by fluorescence microscopy obtaining good photos (*see the fluorescence images of the SH-SY5Y tumor cell line in the APPENDIX 2*).

4.4. Fluorescence microscopy studies of the interaction between MNPs:anti_CDs and the targeting of CSCs with these antibody-functionalized MNPs

The goal of these essays was to optimize the conditions for achieving the maximum interaction between NPMs and anti-CDs, and thus reaching together the target (the CSCs) with the maximum guarantees. As already discussed, the labeling of MNPs with anti-CDs is a

crucial step for the selective and specific labeling of the CSCs within the tumor. Therefore, an experiment to study the interaction between MNPs and anti-CDs in different media, mimicking the behavior of these conjugates in hypothetical living conditions which would be found inside of blood stream, was designed. After doing several initial essays without satisfactory results, possibly *because this functionalization method chosen, by electrostatic interactions, does not seem sufficiently consistent to take account in carrying out more complex essays such as when it works in PBS or cRPMI* it was decided to simplify the experiment. In doing so, several essays working in basic conditions (TRIS buffer pH:7.9) were evaluated to study the affinity between MNPs:anti-CDs *(explained in the experimental section 3.2.4.)* [*see the FIG. 8*].

The **functionalization process** was carried out by electrostatic interactions *[see the FIG. 3]*, where the carboxyl groups of the FcR of the anti-CDs were made interact with the free amine groups on the surface of the MNPs. Both anti-CDs, anti-CD44 and anti-CD133, have an isoelectric point of 7.3, therefore, the carboxyl groups present negative charge for this pH and for more basic values. For the case of the MNPs the isoelectric point (Zeta potential) is 9.2, so the closer the pH value are to 9.2, the more positive charges the MNPs have on the surface (reason because the TRIS buffer pH:7.9 was chosen). Moreover, thanks to the interaction between the anti-CDs and the MNP is realized in the FcR, the Fab region is free to interact with the CSCs markers (fundamental step). In principle, these electrostatic interactions achieved will remain at the physiologic pH, 7.3 (blood conditions), disappearing for lower values because of the protonation of the carboxyl groups (loss of the negative charges).

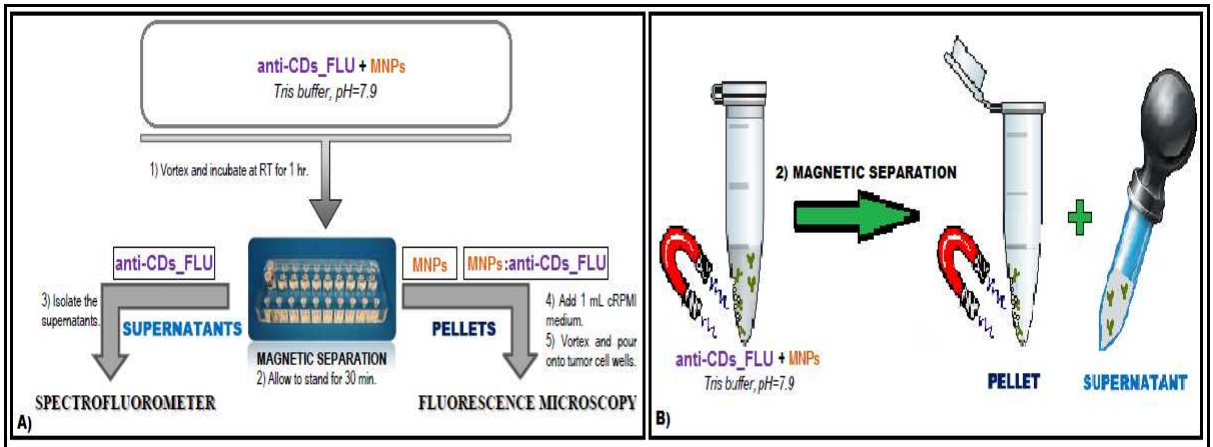

FIG 8. Study of the interaction between MNPs:anti_CDs at pH basic conditions. The samples were analyzed by spectrofluorometer and fluorescence microscopy. **A)** Scheme of the experiment. The photo corresponds to this experiment. **B)** Detailed scheme of the process of separation by magnetic column (Magnetopure size big [Chemicell]).

Once the magnetic separation was carried out, after the incubation process between the anti-CDs and the MNPs, two types of samples were collected: *Supernatants* and *pellets*. **The observation of a loss of anti-CDs in the supernatants with the resultant presence of them in the pellets will corroborate the affinity between the MNPs and the anti-CDs. Besides, the incubation of these MNPs:anti-ABs_FLU with the tumor cells will allow to locate the CSCs inside the tumor sample.**

On the one hand, the **supernatant samples**, containing the anti-CDs_FLU unreacted free from the MNPs or MNPs:anti-ABs_FLU, were obtained. According to our estimates, the peak intensity for each of these sample (measured by the spectrofluorometer) should be lower gradually, meaning a less amount of anti-CDs in the supernatant since they will have reacted with the MNPs, for higher values of the MNPs concentration (added during the incubation). This is because a higher amount of MNPs permits an increased interaction surface for the anti-CDs. The hypothesis seems to be fulfilled in outcomes obtained in the graphic *[represented in the FIG. 9]*. Specifically, this is true for all the samples except for the sample which had been incubate with the highest MNP concentration. An adequate MNP concentration there might be, in this case around 50 µg mL^{-1}, producing the MNPs agglomeration for higher concentrations and avoiding the interaction between MNPs and anti-CDs_FLU. Besides, the affinity between MNPs and anti-CDs seems to change slightly for anti-CD44 or anti-CD133, because the agglomeration effect previously described is lower in the case of the first anti-CD.

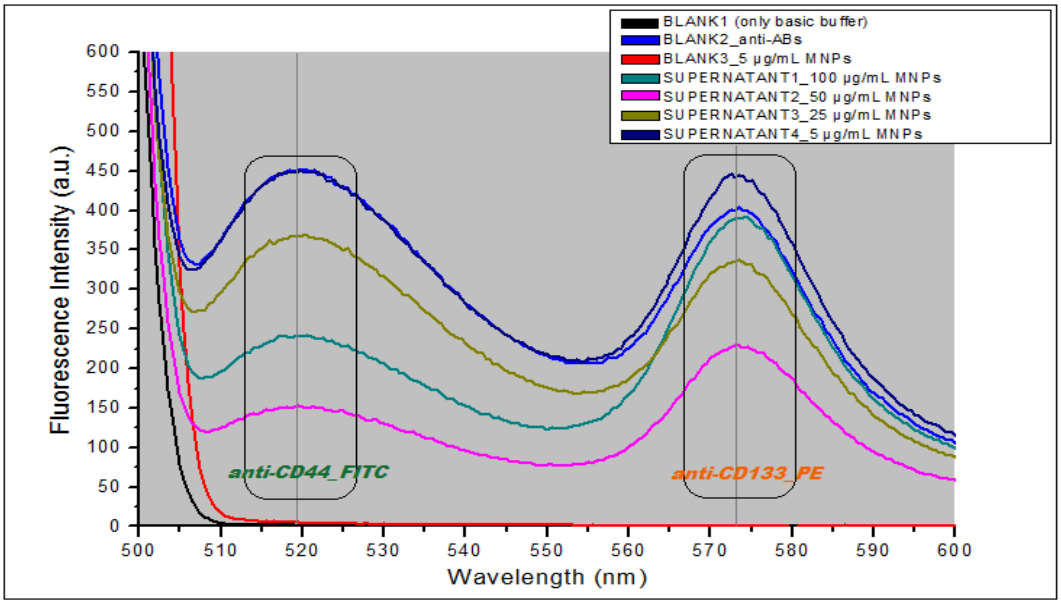

FIG 9. FLUORESCENT SPECTRUM OF THE SUPERNATANTS. Study of the interaction between MNPs:anti-ABs in tris buffer, pH:7.9. 10 µL of each anti-CD44_FITC and anti-CD133_PE were added for every sample. *Data taken by Perkin Elmer LS5S Fluorescence Spectrometer.*
Note:The concentrations of MNPs shown in the legend correspond to the previous step,since the supernatants are MNPs-free.

On the other hand, the **pellet samples** were obtained, containing the magnetic species (MNPs and MNPs:anti-CDs_FLU), free from the anti-CDs_FLU unreacted. These pellets were also attempted to analyze by spectrofluorometry without results, possible due to a quenching effect by MNPs. For that, a new hypothesis was proposed, consisting to incubate the pellets with a tumor cell line, trying to detect the fluorophores by fluorescence microscopy. *The results were positive, as shown in the pictures of the FIG. 10, for the case of the anti-CD44_FITC, but without results for anti-CD133_PE. Thanks to this essay was to demonstrate (only for the anti-CD44) that the interaction had occurred and, moreover, and conclusively proven to targeting the CSCs for the human neuroblastoma cell line SH-SY5Y* [*see the FIG 10*]. The images shows some blanks prepared and the results for the pellet samples, 5 and 25 μg mL^{-1}, after incubating the pellets with the tumor cell. The blue color present in some pictures corresponds to the DAPI which is used extensively in fluorescence microscopy since this is a fluorescent stain that binds strongly to A-T rich regions in DNA, allowing to clearly locate cells. The green color is the anti-CD44, which is present in many cells of every sample. *Unfortunately, the anti-CD133 was not observed, even for the dynamic range also studied, decreasing the intensity to the minimum (extreme conditions) as shown in the picture 3.d of the FIG.10.*

The same experiment was repeated using a different fluorescence microscope, obtaining the same results (*see the fluorescence images of the SH-SY5Y tumor cell line in the APPENDIX 2).*

Concretely, the goal was to localize specifically the CSCs at the junction of both anti-CDs_FLU, since neither of them alone is specific for the CSCs, but unfortunately one of them did not work. The causes of this problem are unknown. On the one hand, it does not appear to be a problem related to a loss of the fluorescence because of it was observed fluorescence by spectrofluorometry. On the other hand, according to the introduction, there exists a sub-population about the 2.7% of CSCs for the SH-SY5Y cell line, using this anti-CD133 marker, therefore, that does not seem to be a problem related to a non-specific CSC marker. Therefore, the real problem might be due to a functionalization loss of the anti-CD133. It must take into account that these anti-CDs_FLU were transported from USA to Spain, remain at room temperature for over 24 hrs (at the end of summer), so it is possible seems feasible that the anti-CD133_PE was damaged.

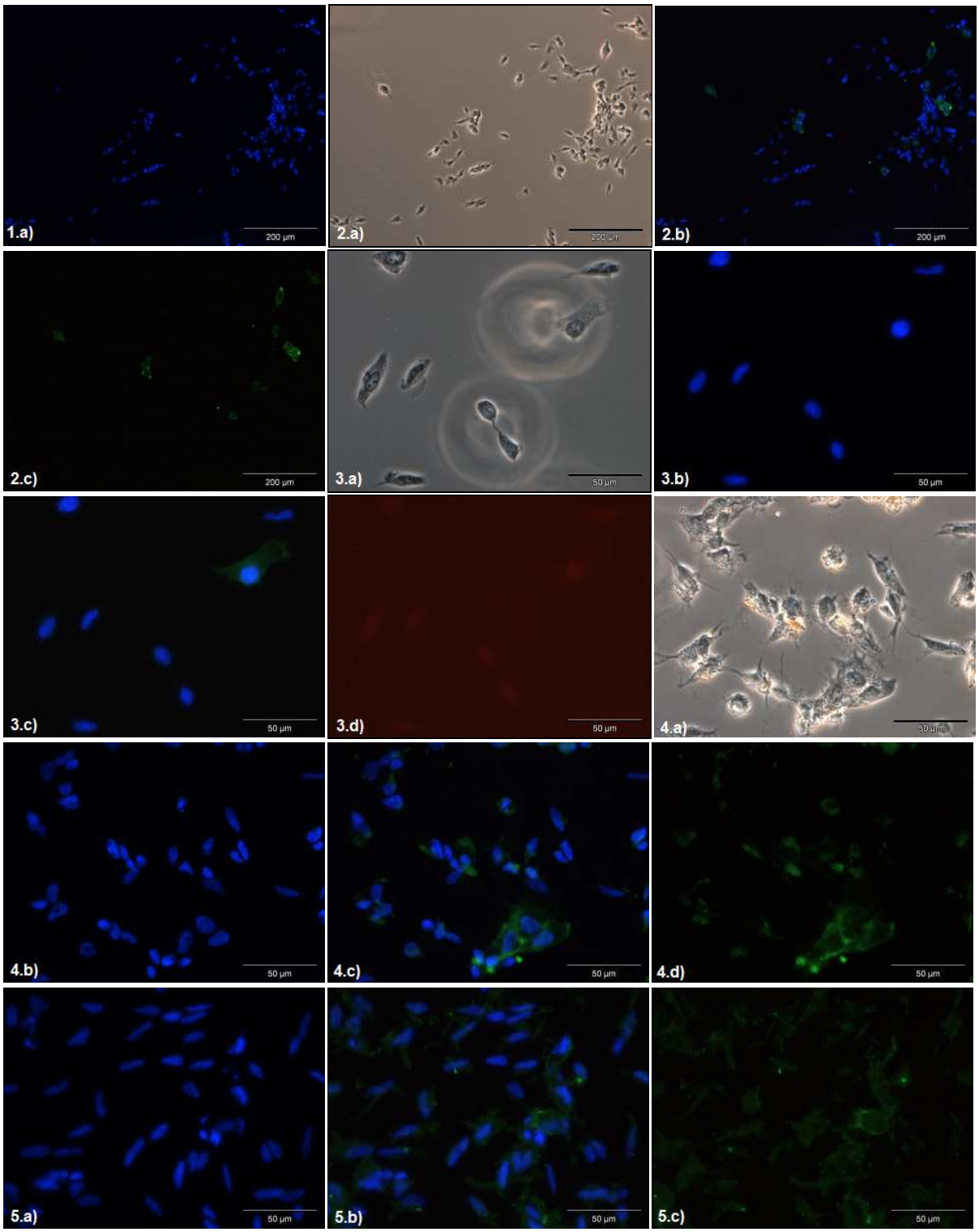

[FIG 10] FLUORESCENCE IMAGES OF THE PELLETS. Study of the interaction between MNPs:anti_CDs in TRIS buffer, pH:7.9. Fluorescence images of SH-SY5Y_pellets (culture medium): **1)** BLANK 1 (only cells), 10X; **1.a)** Cells (DAPI). **2)** BLANK 2 (cells + anti-ABs), 10X; **2.a)** Cells, **2.b)** Cells (DAPI)_anti-CD44_FITC, **2.c)** Cells_anti-CD44_FITC. **3)** BLANK 2 (cells + anti-ABs), 20X; **3.a)** Cells, **3.b)** Cells (DAPI), **3.c)** Cells (DAPI)_anti-CD44_FITC, **3.d)** Cells_anti-CD133_PE (dynamic range). **4)** SUPERNATANT 4: 5µg mL^{-1}, 20X; **4.a)** Cells, **4.b)** Cells (DAPI),4.c) Cells (DAPI)_anti-CD44_FITC, **4.d)** Cells_anti-CD44_FITC. **5)** SUPERNATANT 3: 25 µg mL^{-1}, 20X; **5.a)** Cells (DAPI), **5.b)** Cells (DAPI)_anti-CD44_FITC, **5.c)** Cells_Anti-CD44_FITC. *Images taken by the inverted fluorescence microscope OLYMPUS IX81, with the help of Dr. María Royo in the microscopy and image service of the IACS (Zaragoza).*

IV. CONCLUSIONS

A set of experiments corresponding to the functionalization of MNPs with anti-CDs, and the CSCs targeting with these compounds formed, has been described. Moreover, it was also fundamental to obtain some preliminary information about cytotoxicity studies or the affinity between this kind of MNPs and the tumor cell lines studied, due to the lack of information of this system (*MNPs-Tumor cell*).

With regard to the cytotoxicity studies, the determination of the cell viability of cultured tumor cells with MNPs by MTT essays were carried out. To that end, these experiments were realized modifying the concentration of MNPs and the times of incubation. The results showed that the cytotoxicity effect of the MNPs on the tumor cell lines studied is minimal, representing a net loss of cell viability about 20% in the range of MNPs concentration studied (0-200 $\mu g\ mL^{-1}$), without causing any appreciable change over time.

Studies related to the surface and intracellular distribution, of the MNPs treated-tumor cells, were then realized. On the one hand, the affinity between MNPs and tumor cell lines was verified by Neubauer chamber counting, confirming that practically all cells attach the MNPs for each tumour line studied (PCI-13, MIA PaCa-2 and MDA-MB-231). On the other hand, thanks to an analysis of the intracellular distribution of the MNPs treated-tumor by SEM technique was corroborated that the cell line SH-SY5Y internalizes the MNPs. Besides, there appears to be that the MNPs alter the tumor cell morphology (a more complex cell surface pattern).

Finally, the synthesis of the fully functional MNPs with highly specific markers and the CSCs targeting of these compounds, by fluorescence microscopies, was carried out. Primarily, the antibody-functionalized MNPs (MNPs:anti_CDs) was characterized in terms of stability and functionality, in basic media, obtaining a stable compound, for both anti-CDs (anti-CD44 and anti-CD44). Furthermore, it was observed as there seems to be an adequate MNP concentration, in this case around 50 $\mu g\ mL^{-1}$, producing the MNPs agglomeration for higher concentrations and, thus, avoiding the interaction MNPs-anti-CDs. Finally, the targeting of CSCs with these previously synthesized complexes was evaluated. Thanks to this essay it was demonstrated, for the case of the SH-SY5Y, that the labeling of CSCs is successful only for the anti-CD44. Unfortunately, the CSCs targeting with the anti-CD133 was not observed, possibly due to a functionalization loss because of the anti-CD133_PE was damaged.

These preliminary studies have provided us a clear idea of the difficulties that we face in the future if we go ahead with this ambitious project. On the one hand, the next step would be to improve the functionalization method used, trying to localize the CSCs with a good anti-CD133, in addition to carry out studies in more complex media. On the other hand, since there is no information available on whether hyperthermia can eradicate CSCs, our future challenges could be to evaluate if CSCs are sensitive to hyperthermia-induced by magnetic nanoparticles, and this may lead to control tumor growth (proliferation). Furthermore, it could also be examined if MHT increases sensitivity of cancer cells lines to chemo and radio therapy due to eradication of CSCs.

Bibliography

[1] M. Forrest et al., Advanced Materials (2011).

[2] R. G. Mckinnell. The Biological Basis of Cancer. Cambridge University Press (2006).

[3] Bonnet D, Dick JE. Nature Medicine. 3(**7**):730-7 (1997).

[4] H. Clevers et al., Nature Medicine. **17**, 313-9 (2011).

[5] N. A. Lobo et al., Annu Rev Cell Dev Biol, **23**, 675-99 (2007).

[6] M. Clarke et al., Cancer Res. **66**, 9339-44 (2006).

[7] M. Prince et al., Proceedings of the National Academy of Sciences of the United States of America (PNAS). **104**, 973-978 (2007).

[8] C. Visus and A. B. DeLeo et al., Cancer Res. **67**: (21) (2007).

[9] S. K. Singh et al., Cancer Research. **63**, 5821-5828 (2003).

[10] S. Chuthapisith et al., Surgical Oncology. **19**, 27-32 (2010).

[11] Sean P. McDermott, et al., Molecular Oncology. 4, 404-419 (2010).

[12] D. G. Heidt, Cancer Research. 67 (3):1030-1037 (2007).

[13] Q. Bao et al., Cancers. **2**, 1629-1641(2010).

[14] H. G. Liu et at., Asian Pacific J Cancer Prev. 10, 177-179 (2009).

[15] Quiang-Song et al., World J Pediatr. 4(1):58-62 (2008).

[16] J. Walton et al., Neoplasia. **6**, 838–845 (2004).

[17] P. Lázcoz et al., Trauma Fund MAPFRE. 19(2):120-127 (2008).

[18] A. Arruebo et al., Nanotoday. 2 (3) (2007).

[19] A. Kumar et al., Nanomedicine. **6**, 64-9 (2010).

[20] I. Brigger et al., Adv Drug Deliv Rev. **54**, 631-51 (2002).

[21] G. Goya et al., Current nanoscience. **4**, 1-16 (2008).

[22] M. shinkai et al., Journal of Magnetism and Magnetic Materials. **194**, 176-184 (1999).

[23] R. D. Issels et al., European Journal Of Cancer. **44**:2546-2554 (2008)

[24] A. Ito et al., Cancer Immunol Immunother. **55**, 320-8 (2006).

[25] A. Chichel et al., Rep Pract Oncol Radiother. 12(5): 267-275 (2007).

[26] J. Zan der Zee et al., Annals of Oncology **13**, 1173-1184 (2002).

[27] A. Arruebo et al., Cancers. **3**, 3279-3330 (2011).

Acknowledgements

The author is grateful to the Dr. Albert DeLeo and the Dra. Carmen Visus for giving him the opportunity to carry out the first part of the project in the Inmunology department at the Hillman Cancer Center of Pittsburgh (USA). He must also thank to the Dr. Gerardo Goya for giving him the chance to perform the second part of this project in the Magnetic Hyperthermia group at the Institute of Nanotechnology of Aragon (INA).

III. EXAMPLE 2: Regioselective control of molecular nanoprobes on filamentous virus particles and self-assembly of these functionalized rod-like nanoparticles

1. INTRODUCTION

Viral nanoparticles (VNPs) form the basis of some novel renewable molecular materials due to many attractive features of the viruses such as a precise nanoscale dimensions, elasticity, stability, low polydispersity, biocompatibility and well known genetic information with an efficient and inexpensive production **[1-3]**.

1.1. M13 bacteriophage: wild type and mutant virus

The filamentous M13 bacteriophage *[see the FIG. 1,2]*, an abundant virus in nature that infects the bacteria E. coli, is an ideal candidate for nanotechnology, among other features because it is non-enveloped, i.e. without a lipid membrane, so the functional groups on the capsid proteins can make direct contact with coating materials. General properties of these rod-shaped viruses include a length of about 900 nm, 6.5 nm in diameter, a molecular weight of $1.6x10^7$ g mol^{-1} and a circular single-stranded DNA genome encased by several phage-encoded proteins. The major protein capsid is a pVIII protein, where approximately 2700 of these coat proteins are helically wrapped to construct the flexible cylindrical body of the bacteriophage. At one end of this protein assembly, five copies of the pIII, a minor coat protein, form the tails of the phage that modulates phage infectivity of the host bacteria **[4-6].**

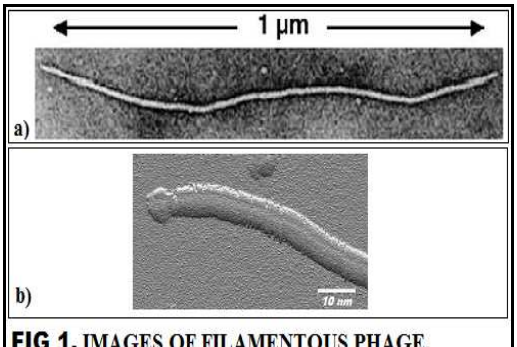

FIG 1. IMAGES OF FILAMENTOUS PHAGE. **a)** Visualized by electron micrograph *[Dogic Z. and Fraden S. et al., 2006]*. **b)** Visualized by atomic force microscopy. The large size of the phage tip structure suggests that it is the pIII end*[The Bacteriophages.Oxford University Press,2006]*.

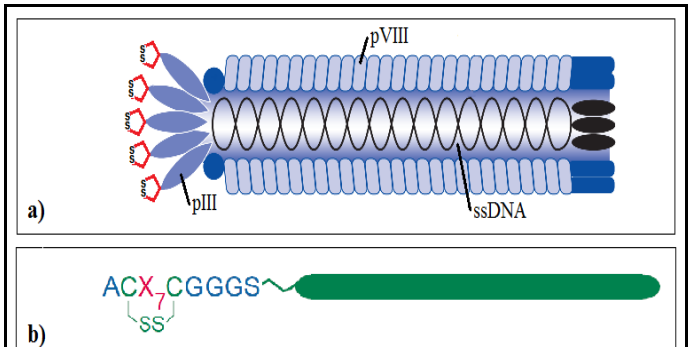

FIG 2. MUTANT M13-C7C PHAGE. a) Linker sequence in each of the 5 copies of the PIII protein clustered at one end of the M13 virus. **b)** Structure of the loop-constrained heptapeptide flanked by a pair of cysteine residues.

These rod-like colloids can be handled easily in the laboratory and have long been used in molecular biology studies because they are amenable to genetic modification of virus capsid proteins. Besides, a very interesting characteristic of these VNPs is that non-reactive cysteine residues are exposed to exterior surface because evolution had disfavored interparticle disulfide bonds. Therefore, this presents a unique opportunity to genetically monitor the position of the cysteine residue on strategic locations of the virus and protein shells, after which the thiol group can be selectively targeted with thiol-selective probes [7].

The mutant M13-C7C bacteriophage *[see the FIG. 2]* is based on a simple M13 phage vector modified, in the end of the pIII protein, by pentavalent display of a loop-constrained heptapeptide. Each loop is flanked by a pair of cysteine residues, which could be oxidized during the phage functionalization to a disulfide linkage. In this case, the infectivity function of PIII is not affected because the displayed peptide is sufficiently short (<50 residues). Furthermore, the LacZ gene has been genetically inserted into the mutant phage vector, which is used as a characterization method to distinguish between the mutant M13-C7C and the M13 (wild-type) phages thanks to the mutant phage plaques appear blue when plate on media containing XGal and IPTG. An important concept in biology is the plaque-forming unit (PFU) which is a measure of the number of particles capable of forming plaques (colonies) per unit volume, such as virus particles. Unfortunately, there exists a counterproductive part resulting in a longer replication cycle of the mutant phage compared with the wild type. As a result, *there is the possibility of in vitro selection for any contaminating wild-type phage during the amplification steps, even vanishingly small levels of contamination can result in a majority of the phage pool* **[8]**.

1.2. Liquid crystalline organization

'Soft' matter, including polymers, colloids, amphiphiles, liquid crystals and a lot of biological systems, presents two fundamental features. The first one, the ordering is generally intermediate between that of a crystalline solid and that of a liquid, and the second one is the range of organization shown in the structures formed, typically in the 'nanoscale' ordering (1-1000 nm). An important distinction between different types of soft material is the difference between direct and indirect ordering of molecules via supramolecular aggregates **[9]**.

Liquid crystals are materials presenting at least one intermediate phase between isotropic liquid and crystalline solid phases. The calamitic liquid crystals are the most

common type of self-assembly for these structures, composed exclusively of anisotropic particles exhibiting a rod-shape. Liquid crystals composed of rod-like colloids exhibit different phase sequences with increasing concentration, behaving as lyotropic liquid crystals. The simplest liquid crystalline phase is the so called nematic (N), in which the molecules are positionally totally disordered, but arrange in a same preferential direction. The Smectic (Sm) phase shows a positional order since the centres of mass are arranged in layers (Sm layers) *[see the FIG. 3]* **[10-12]**.

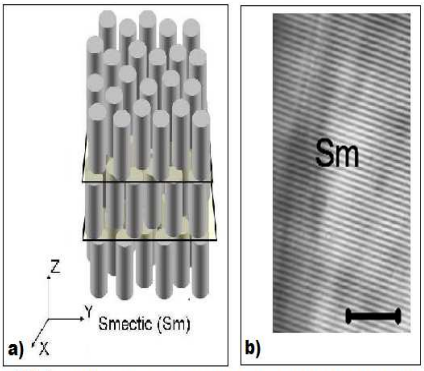

FIG 3. SMECTIC (Sm) PHASE OF LIQUID CRYSTAL. **a)** Schematic representation of the Sm phase of rodlike particles. **b)** Sm or lamellar phase observed by DIC microscopy (digitally enhanced picture). The scale bar indicates 10 µm. *[GRELET E. et al., 2008]*

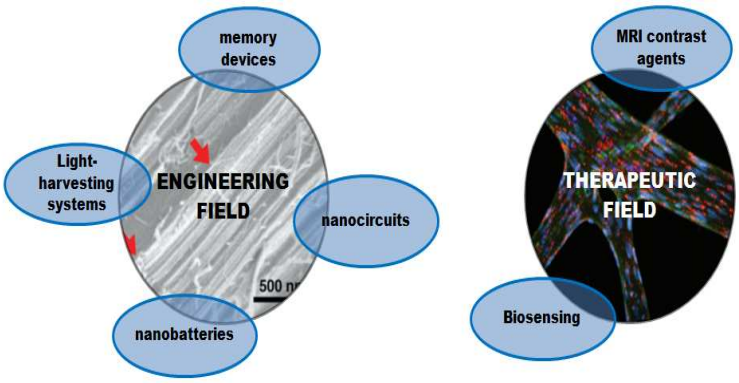

FIG 4. VIRAL NANOPARTICLES (VNPs) APPLICATIONS. Some potential applications for these virus-based hybrid materials for the engineering of therapeutic fields are shown in both diagrams. **PICTURES**: **(left)** SEM image showing the close-packed lamellar structure of phage and nanocrystal layers (red arrows) in the inner areas of the film *[S-W. Lee, A. M. Belcher et al., Science. Vol 296 (2002)]*. **(right)** Intravital Imaging of Human Prostate Cancer Using Viral Nanoparticles *[N. F. Steinmetz et al., Small. Volume 7, Issue 12, pages 1664–1672 (2011)]*.

1.3. Applications of the virus-based hybrid materials

There exists an ample utilization of the phage display technology for material science applications. Liquid crystalline self-ordering systems with nanosized features of engineered viruses may provide new pathways to organize electronic, optical, and magnetic materials that would not be feasible via the traditional top-down fabrication techniques **[3, 13]**. For example, the wire-structures of viruses have inspired studies of their applications as conductive nanowires for electrical devices such as nanocircuits or nanobatteries, by mineralizing continuous metal layers on the virus surface, to obtain nanowires that exhibit crystallographic ordering **[4]**. Also, studies of the use of rod-like viruses as biological scaffolds for the construction of light-harvesting systems or magnetic systems are noteworthy both for their potential uses in solar cells, photocatalysts, and optical sensors or memory devices, respectively *[see the FIG. 4 (left)]* **[5]**.

More recently, nanometer-sized constructs, such as dendrimers, liposomes, nanoshells, nanotubes, nanoemulsions, quantum dots, and even viruses are being developed to increase detection sensitivity and efficacy for therapeutic applications as bioimaging agents intended as noninvasive probes (near infrared fluorescent dyes, magnetic contrast agents) or to target biomarkers of disease **[7, 14**]. For example, the crystalline phase of the VNPs could be adjusted to create enhanced suspension stability for magnetic resonance imaging (MRI) contrast agents **[5]**. Also, the VNPs could be an invaluable tool to improve detection, early and accurate biosensing, of small lumps of cancer cells. These "smart" nanoparticles were equipped with bright fluorescent dyes for imaging and a chemical tags to help it find and latch onto cancer cells to increase imaging sensitivity *[see the FIG. 4 (right)]* **[15]**.

2. AIMS

The validation of a method to carry out the mass production of the mutant M13-C7C phages and the optimization process to functionalize with any maleimide probe are reviewed in this work:

- **Amplification, purification and characterization of the M13-C7C phages**. The growth of viruses by M13-C7C-infected bacteria solution and analysis of the phages obtained, by titration process and transmission electron microscopy (TEM), will be carried out.

- **To functionalize phages with nanoprobes**. The functionalization of these rod-like particles, with a previously disulfide reduction process, and labeling with maleimide-functionalized fluorophores of the M13-C7C phage will performed.

- **Self-organization studies**. Liquid crystal line phases will be studied by fluorescence and differential interference contrast microscopy (DIC), in order to validate our scientific approach, i.e. the regioselective functionalization of viral nanoparticles (VNPs).

3. EXPERIMENTAL SECTION

▫ Note: In the *APPENDIX 2* are shown some protocols for working with phages.

3.1. Precautions. It is important to note the special precautionary measures that were taken into account in every step before and during the amplification process always to prevent the contamination of the mutant viruses with the undesired wild-type ones. Basically, the multiplication of the wild type is many times greater than the mutant viruses and consequently the slightest contamination would lead a guaranteed failure. Therefore, the first step was to disassemble and thoroughly clean the micropipettes with 70% EtOH, which were used exclusively in the inoculation processes. Besides, some considerations such as the thorough cleaning of the laminar hood with 70% EtOH every time was used, the use of virgin bacterial culture Petri dish without a previous bacteria extraction or the opening of a new box of aerosol-resistance tips for each new amplification, were strictly undertaken **[8]**.

3.2. M13-C7C amplification process. A volume of LB was inoculated with the mutant M13-C7C solution at a concentration of 10^{11} pfu mL^{-1} (1mL/L for the infecting solution and 0.5 mL/L for the mass production). At the same time, a volume of E. coli ER2738 culture (10mL/L for both cases), previously grown overnight, were also added. The mix was shaken at 37ºC, 230 rpm for different incubation times (5 hrs for the infecting solution and 8 hrs. for the mass production) **[8, 16]**.

3.3. M13-C7C titration process. Firstly, 200 µL of serial dilutions of M13-C7C phage in LB were prepared into sterile tubes. After, 200 µL of E. coli ER2738 (OD_{599}=0.5) were put into each one of the M13-C7C serial dilutions, vortex and incubate for 5 min at room temperature. Then, 3 mL of top agar at 56ºC were also added, vortex and the mix were poured on the top of the IPTG/XGal_LB-agar plates prepared previously. Finally, let cool down, cover with parafilm and grow overnight at 37ºC **[8, 16]**.

3.4. Functionalization process. 50 mL of the M13-C7C mass production (1 mg mL^{-1}) in 20 mM Na_2HPO_4 buffer pH 7.0 was reduced with 1.22 µM TCEP·HCl about 30 min at room temperature. Then, the solution was mixed with 3.05 µM of DyLight 550 Maleimide (*1 mL of DyLight 550 Sulfhydryl-Reactive Dye purchased from the Thermo Scientific Company*) dissolved in DMSO, $1:10^4$ dilution to prevent virus damage, stirring gently it at 4ºC for 2 hrs. It must be taken into account that is needed 10 times more of reduction agent and dye per virus molecules, because there are 5 tails per M13-C7C molecule with 1 disulfide group in each tail. Besides, it has been used about 2 and 8 molar excess of reduction agent and dye, respectively **[17-19]**.

4. RESULTS AND DISCUSSION

▫ Note: *In the APPENDIX 2 are shown some photos taken during the course of the project.*

4.1. BIOLOGY

Before starting the experiments, a 1:100 dilution of the M13-C7C bacteriophage (*100 mL of Ph. D.-C7C [phage display Library], ~10^{13} pfu mL^{-1}, purchased from the New England Biolabs Company*) was prepared, because a 10^{11} pfu mL^{-1} value is required for the amplification process.

The first step was to prepare 50 mL of the **infecting solution**, corresponding to a first amplification, needed to carry out subsequently the M13-C7C mass production. It was mandatory to check the complete absence of wild type viruses (M13 phages) in the infecting solution before to proceed with the following steps. *In the FIG. 5* are shown four filamentous phages with an estimated length of 1006 nm (accomplished by Alexis de la Cotte of the CRPP). Many impurities are observed in the picture due to the LB medium drying.

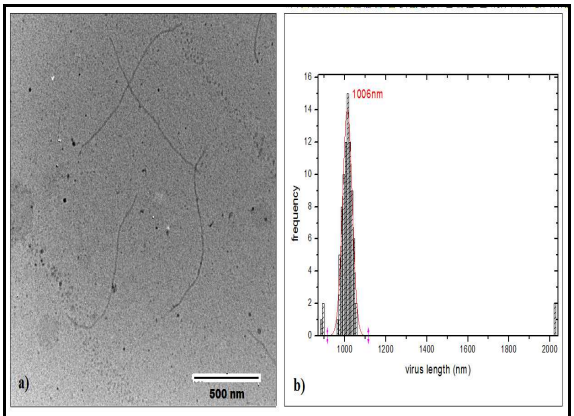

FIG 5. TEM. **a)** Image of the M13-C7C phages. **b)** Virus length calculated from 95 independent photos. *Images taken by the H600 Hitachi TEM. The images and the analysis of data were realized by Alexis de la Cotte (CRPP).*

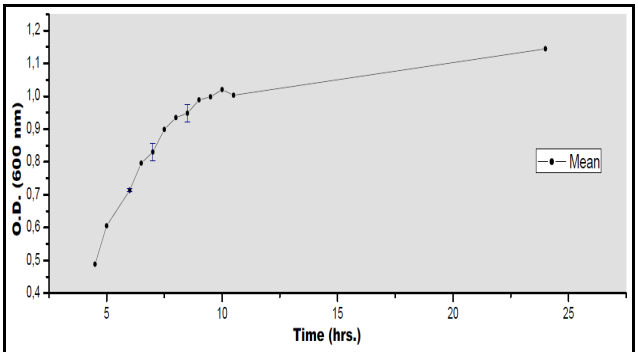

FIG 6. OPTIMIZATION OF THE M13-C7C AMPLIFICATION PROCESS. Optical Density (O.D.) measurements at different incubation times were taken to study the bacteria growth. The results indicate that the exponential phase corresponds to about 10 hours. *The data and error bars represent the mean and standard deviation (SD) of n=2 independent experiments.*

An **optimization process** was now realized to optimize the steps of multiplication and purification needed for the mass production. Specifically, Optical Density (O.D.) measurements at different incubation times were taken to study the bacteria growth curve *[see the FIG. 6]*. Viruses need to infect bacteria to multiply. Therefore, virus amplification also occurred during bacterial amplification, corresponding to the exponential phase. The results indicate that the exponential phase before it reaches the plateau (stationary phase) is between 4 and 10 hrs. It should be noted that the probability of infecting the amplification solution

with the wild type viruses increases with incubation time, due to a higher number of mutations. After several amplifications essays, it was confirmed that a suitable amplification time is 8 hrs. Besides, the purification process was also maximized, adapting the centrifugation steps (times and speeds) *[see the FIG. 7]*.

Once the process was optimized, the **M13-C7C mass production** was carried out to produce the M13-C7C in huge amounts. For do that, 10 independent experiments of amplification with a final volume of 2 L were made to obtain about 284 mg of the mutant M13-C7C phage, free from wild type *(see the experimental section 3.2.)*.

A **purification process** of the M13-C7C phages is needed to carry out after each amplification process. This process is composed of a depletion step and several centrifugation steps *[see the FIG. 7]*, which aims is obtain the M13-C7C in high concentration diluted in dH_2O and free of bacteria, LB and other impurities.

These last two processes, the amplification and purification, are the most important steps in the work, consequently where more time has been invested, because a large-scale production of pure mutant M13-C7C viruses is necessary to form smectic phases of liquid crystals.

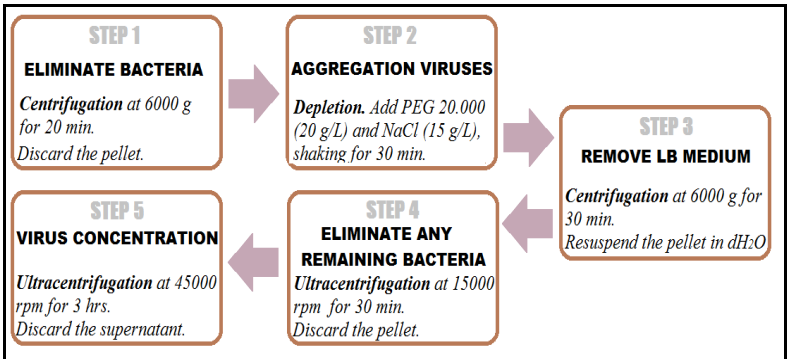

FIG 7. *M13-C7C PURIFICATION PROCESS.* This process is composed of several centrifugation steps, all carried out at 4ºC, which goal is to obtain the M13-C7C in a high concentration diluted in dH_2O and free from bacteria, LB and other impurities. *The ultracentrifugation steps carried out by the Thermo Scientific SORVALL WX Ultra series centrifuge with F50L-8x29 rotor.*

FIG 8. M13-C7C TITRATION PROCESS. Results obtained where blue plaques are observed into the plate.

Finally, a **checking process** by titration was carried out for each sample amplified *(explained in the experimental section 3.3.)* to corroborate that the amplification had been successful *[see the FIG. 8]*. Specifically, this characterization process allows to know both

whether or not the amplified culture is infected, by the wild type M13, and the PFU mL^{-1} value.

The results achieved were satisfactory, even exceeding our expectations, obtaining considerable amounts of M13-C7C with only blue colonies in all plates. To confirm of absolutely way that the viruses correspond exclusively to mutant M13 an amplification of DNA is suggested ***[8]***. But this process is only suitable when it works with analytical quantities. Therefore, the functionalization of the mutant M13-C7C bacteriophages with fluorescent probes and the study the liquid crystalline phases obtained will be done to confirm in a definitive way these biological results.

4.2. CHEMISTRY

The second part, the chemistry, a functionalization method was proposed both to validate the amplification process, to verify this once and for all and also to validate this functionalization method.

After the functionalization process *[see the FIG. 9]*, composed of a first reduction step of thiol groups and another corresponding to the labeling with the 550 maleimide dye (*explained in the experimental section 3.4.*), two dialysis processes were carried out. Firstly, with dH_2O to remove the excess of dyes and the second with 20 mM TRIS, pH 8.1, 20 mM NaCl, to change the pH for suitable working conditions with virus liquid crystals.

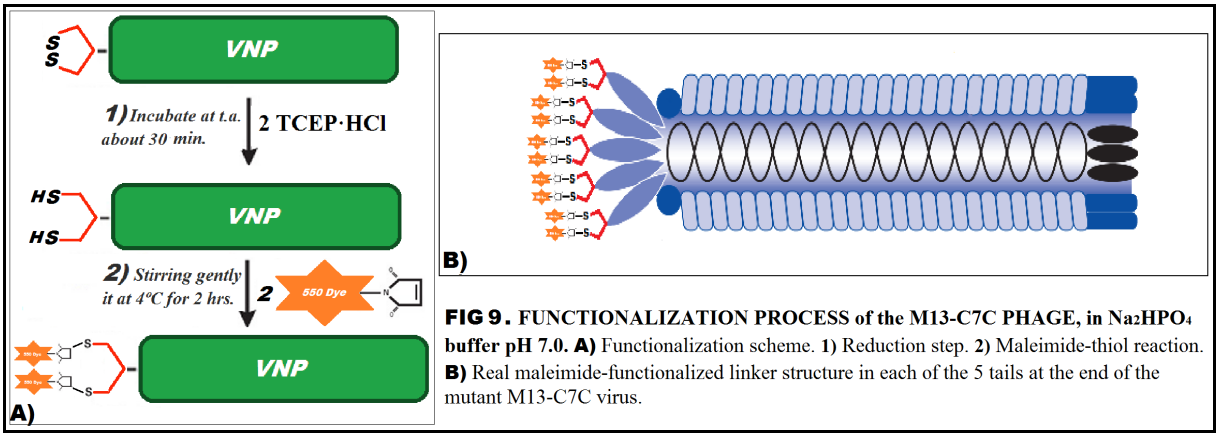

FIG 9. FUNCTIONALIZATION PROCESS of the M13-C7C PHAGE, in Na_2HPO_4 buffer pH 7.0. A) Functionalization scheme. **1)** Reduction step. **2)** Maleimide-thiol reaction. **B)** Real maleimide-functionalized linker structure in each of the 5 tails at the end of the mutant M13-C7C virus.

It is noted that in this **purification step**, corresponding to dialysis step, did not work to remove the excess of dyes for both dH_2O and TRIS buffer. This is because a pink solution,

corresponding to the dye color in solution, was not obtained after the first dialysis step. Despite that, the dialysis process is needed to remove protein remains and other impurities that are impossible to remove by centrifugation. Therefore, to overcome this obstacle and to remove the excess of dye, several ultracentrifugation steps were carried out.

4.3. PHYSICS

An ultracentrifugation process was fundamental, in any case, to concentrate the viruses for the **sample preparation**. Working with liquid crystals, and study the smectic (Sm) phases, must be achieve concentrations around 90-140 mg mL^{-1} of virus. To do this, the sample preparation is a delicate and laborious process, because we need homogeneous sample which is highly concentrated. The iridescence phenomena, due to visible light diffraction of the smectic layers (having a periodicity of about 1 μM), were observed within the sample once a homogenous smectic phase is achieved *[see Appendix, the Image 12]*.

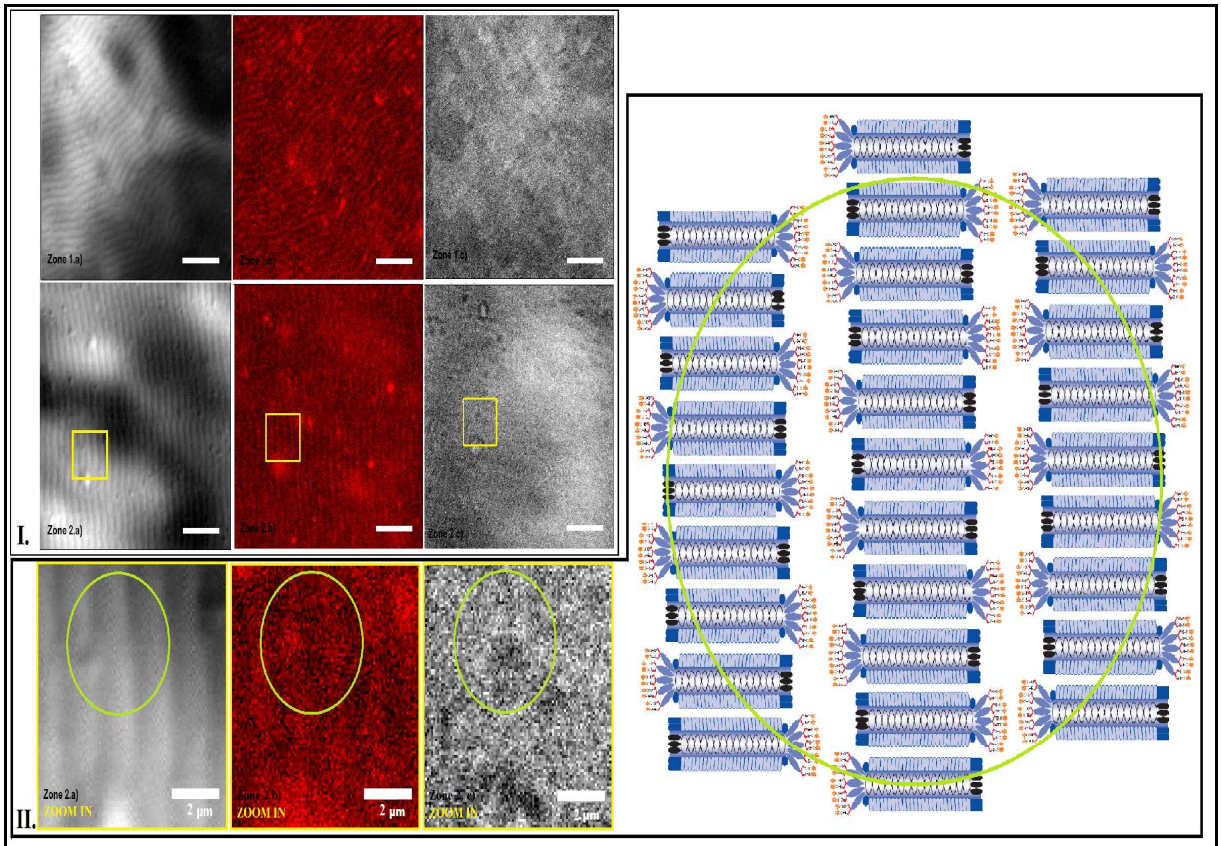

FIG 10. LIQUID CRYSTAL STUDIES. I. Smectic (Sm) or lamellar phages, of the M13-C7C phages, observed in two different zones in the same sample. The scale bar indicates 6 μm (digitally enhanced pictures): **a)** DIC; **b)** Fluorescence image, Ex:550 nm; **c)** Fluorescence image, Ex:488 nm. **II. (left)** The same subarea for the zone 2 has been extended for the three cases studied. **(right)** Self-organization scheme for the mutant M13-C7C phages, inside the studied subarea, where each line corresponds to a layer of viruses. *Images taken by LEICA DMIRE2 confocal microscope.*

Self-organization studies. Three images of the smectic phases, using different observation conditions, in two different zones were taken by confocal microscopy *[see the FIG. 10]*. Clear lines are observed by differential interference contrast (DIC) microscopy. Each line corresponds to a layer of virus with a width of the size of the M13 virus (1.006 μm). Two different results are obtained when the fluorescence is measured. On the one hand, exciting at 550 nm our 550 DyLight emits red light, showing the functionalized tails colored. On the other hand, it is not observed the pattern of lines in the sample when the sample is excited at 488 nm. This confirms that the goal has been achieved, obtaining phages functionalized with fluorophores with a regioselective control. Besides, thanks to this functionalization step it could verify that the amplification process was a success.

An important consideration, constituting the most direct application of our results, is that an optical technique more easily available in any lab, such as fluorescence microscopy, can be now used to study these self-organization structures. Therefore, it is not already necessary to use an advanced technique, such as DIC, to observe the Sm or lamellar phases whenever working with these fluorescence mutant M13-C7C viruses.

5. CONCLUSIONS

A simple approach for the mass production of mutant M13-C7C viruses by amplification process, free of the wild type, is described. The main advantage of this M13-C7C amplification process is the large-scale production of the mutant phages exhibiting cysteine residues at one of its extremities. However, the special precautionary measures to be taken to avoid any contamination with the wild type viruses, before and during the amplification process, are strong. Herein lies the importance of this method validated, namely the neatness worked with over the life of this project.

With regard to the biology part, the first challenge was to obtain the infecting solution, without the M13 viruses, and perform the optimization process. Secondly, the multiplication processes, with the corresponding purification steps, were carried out many times until a sufficient quantity of mutant viruses were reached. The results achieved were more than satisfactory obtaining considerable amounts of mutant M13-C7C viruses. To do

this, a checking process by titration was carried out, obtaining exclusively blue colonies for each phage dilution on every plate.

The chemistry section consisting in a method of functionalization was then realized, achieving the validation of this method as well as definitively the amplification process also. To do this, a first reduction step of thiol groups and another corresponding to the labeling with a maleimide dye, with the corresponding purification steps, were realized.

Finally, related to the physics part, the self organization studies of these functionalized rod-like nanoparticles were carried out. To that end, the sample was prepared through a delicate process. Three images of the smectic phases, using different conditions, were taken by confocal microscopy. Bright lines, each corresponding to a layer of virus were observed by differential interference contrast (DIC) microscopy. Two different results, exciting at 550 nm or 488 nm, were obtained when the fluorescence was measured, showing the functionalized tails colored due to a pattern in the sample or non-pattern observed, respectively. This confirms that the aim was achieved, obtaining phages functionalized with fluorophores with a regioselectivity control.

Over the years noticeable advances are being made in the fabrication of nanostructured novel materials from VNPs due to the unique capabilities of the viruses, such as high monodispersity, chemical specificity and the anisotropic character. We anticipate that our approach, using a liquid crystalline self-ordering system of engineered mutant viruses, may provide new pathways to organize electronic, optical, and magnetic materials among other potential applications. Therefore, our next challenge could be to develop hybrid materials formed by the monitored assembly of these mutant M13-C7C phages with magnetic nanoparticles, with a 1:1 molar ratio, to induced highly sensitive nanorods by magnetic field.

Bibliography

[1] J. Pokorski et al., Mol. Pharmaceutics. **8** (1), pp 29–43 (2011).

[2] K. Koudelka et al., Current Opinion in Chemical Biology. **14**, 810–817 (2011).

[3] S-W. Lee, A. M. Belcher et al., Science. Vol 296 (2002).

[4] C.M. Soto et al., Current Opinion in Biotechnology. **21**, 426–438 (2010).

[5] S. Lee et al., Biotechnology and Bioengineering, Vol.109, Nº.1 (2012).

[6] The bacteriophages. Oxford University Press (2006).

[7] L.A. Lee et al., Org. Biomol. Chem. **9**, 6189 (2011).

[8] Ph.D.™-C7C New England BioLabs. PhD Phage Display Libraries.

[9] I. Hamley et al., John Wiley & Sons (2007).

[10] P. Collings, Introduction to liquid crystals, Taylor & Francis (1997).

[11] Z. Dogic and S. Fraden, Current Opinion in Colloid & Interface Science, **11**, 47-55 (2005).

[12] E. Grelet, Physical review letters. **100**, 168301 (2008).

[13] L.A. Lee et al., Nano Res **2**, 349-364 (2009)

[14] S.D. Caruthers et al., Current Opinion in Biotechnology. **18**, 26–30 (2007).

[15] N. F. Steinmetz et al., Small. Volume 7, Issue 12, pages 1664–1672 (2011)

[16] J. Sambrook, E.F. Fritsch and T. Maniatis, Molecular Cloning. A laboratory manual. Second edition (1987).

[17] M. Brinkley et al., Bioconjugate chem. **3**, 2-13 (1992).

[18] Thermo Scientific, TCEP-HCl. Instructions.

[19] Thermo Scientific, Sulfhydryl-Reactive dyes. DyLight 550 Maleimide. Instructions.

Acknowledgements

The author is grateful for the financial support from the Trans-Pyrenees Action on Advanced Infrastructures for Nanosciences and Nanotechnology (Train2). He would also like to thank both the Dr. Eric Grelet and the Dr. Thierry Michon for giving him the opportunity to carry out this whole project in the Centre de Recherche Paul Pascal (CRPP), CNRS Bordeaux and the Institut National de la Recherche Agronomique (INRA) of Villenave d'Ornon (France), respectively.

IV. GENERAL CONCLUSIONS

Those conclusions specifically related to the results from each subsections (i.e., CSCs and viral particle functionalization) have been already exposed at the end of the corresponding chapters. Here, the general conclusions from the whole work are to be presented.

The work realized along this Final Master project can be evaluated within the framework of two independent research lines on the functionalization of nanoprobes for biomedical or technological applications, respectively.

A first, methodological consideration based on the work and discussions found along several months of this work, refers to the multidisciplinary nature of the research presented here. This multidisciplinary character of our work is the fundamental reason why it has been developed at several different research groups, which were formed by physicists, chemists, biochemists and medical doctors.

The relevance of the nano-object based functionalization has become clear in both applications reported here:

On one hand, with regard to the functionalization method chosen for application to cancer stem cells, the ‘simple’ electrostatic interactions tuned by adjusting the pH gave satisfactory results regarding the functionalization of the MNPs with the anti-CDs. If more complex essays are to be performed in the future (e.g., further change to cRPMI medium or for the actual in vivo conditions), then a more appropriate strategy should be to change for a more robust attachment of the functional groups, such as avidin-biotin or maleimide-thiol binding.

Regarding the second example, i.e. the functionalization of viral particles, the maleimide-thiol functionalization has proven to be an excellent method. The advantages of this method include a strong attachment (covalent bond), high selectivity (reacting exclusively with thiol groups), stability in extreme conditions and simple experimental protocol (it has been developed as a single-step protocol).

It is clear that the age of the nanobiotechnology has just begun. The increasing complexity of diverse materials involving multiple scales, the combination of rational design and evolution, and the emerging confluence of bio and nano are broad technological trends that will give great momentum to nanobiotechnology in the coming years.

○ *ABBREVIATIONS:*

AB: Monoclonal antibody (specific)

anti-CD: Monoclonal antibody (specific)

anti-CD_FLU: Fluorophore conjugated to anti-CD

anti-CD44: CD44 (HI44a) Antibody

anti-CD44_FITC: FITC conjugated to CD44 antibody

anti-CD44_PE: PE conjugated to CD44 antibody

anti-CD133: CD133/1 (AC133) Antibody

anti-CD133_FITC: FITC conjugated to CD133/1 antibody

anti-CD133_PE: PE conjugated to CD133/1 antibody

CD: Surface Cell Receptor or Antigen (CD44 or CD133)

CD44: A highly glycosylated type-I transmembrane cell surface receptor protein

CD133: A glycosylated transmembrane cell surface antigen

cRPMI: Complete medium

CSCs: Cancer Stem Cells

DAPI: 4',6-diamidino-2-phenylindole

DIC: Differential Interference Contrast

DMF: N,N-Dimethylformamide

DMSO: Dimethyl sulfoxide

FcR: Fc receptor

FITC: Fluorescein isothiocyanate

FLU: Fluorophore (FITC or PE)

IPTG: Isoprophyl thiogalactoside, or isopropyl β-D-galactopyranoside

LB: Luria-Bertani broth

M13: A wild-type filamentous bacteriophage

M13-C7C: A mutant form of the M13.

MDA-MB-231: Breast cancer cell line

MHT: Magnetic Hipertermia

MIA PaCa-2: Pancreatic cancer cell line

Milli-Q: Ultrapure water of type 1

MNP: Magnetic Nanoparticle

MNPs:anti-CD: MNPs conjugated to an anti-CD

MNPs:anti-CD_FLU: MNPs conjugated to an anti-CD_FLU

MNPs:anti-CD133_FITC: MNPs conjugated to an anti-CD133_FITC

MNPs:anti-CD133_PE: MNPs conjugated to an anti-CD133_PE

MNPs:anti-CD44_FITC: MNPs conjugated to an anti-CD44_FITC

MNPs:anti-CD44_PE: MNPs conjugated to an anti-CD44_PE

MRI: Magnetic Resonance Imaging

MTT: 3-(4-5-Dimethylthiazol-2-yl)-2,5-diphenyltretazolium bromide

NP: Nanoparticle

PBS: Fetal Bovine Serum

PCI-13: SCCHN cell line

PE: R-Phycoerythrin

PEG: Polyethylene glycol

PEI: Polyethylene imine

PFA: Paraformaldehyde

PFU: Plaque-forming unit

RPMI: Roswell Park Memorial Institute medium

RT: Room temperature

SCCHN: Squamous Cell Carcinoma of the Head and Neck

SEM: Scanning Electron Microscopy

SH-SY5Y: Human neuroblastoma cell line

Sm: Smectic phase

TCEP: Tris-(2-carboxyethyl)phosphine hydrochloride

TEM: Transmission Electron Microscopy

TRIS: Tris(hydroxymethyl)aminomethane

VNPs: Viral Nanoparticles

XGal: 5-Bromo-4-Chloro-3-indolyl-β-D-Galactopyranoside

■ ***APPENDIX 1***

▪ *PROTOCOLS FOR WORKING WITH TUMOR CELLS*

The following steps were undertaken whenever a new essay with tumor cells was launched.

• Some important considerations to take into account when working with cell lines:

- Pre-warmed culture medium and PBS at 37ºC are used.
- It must work under sterile conditions within laminar flow hood whenever an incubation process is carried out later. Therefore, it is also obligatory to use sterile material and sterilized solutions in these cases.
- The cell samples with MNPs must be treated very careful because even the slightest jolt could produce the detachment of cells, because of the shearing stress caused by the MNPs.
- cRPMI: The following compounds must be added to each new RPMI 1640 bottle (Sigma-Aldrich): 10% PBS, 1% L-glutamine, 1% Penicillin/Streptomycin solutions, 1% MEM non-essential amino acid and 1% Sodium pyruvate (100 mM).

• Preservation (or storage) and thawing of tumor cell lines

Liquid nitrogen is used to preserve cultured tumor cells to -196°C. To minimize the effects of freezing, a cryoprotective agent which lowers the freezing point, DMSO, is added. It was used a typical freezing medium composed of 90% serum and 10% DMSO.

The frozen samples of cultured tumor cells were thawed by placing the vials directly into a 37°C water bath. As soon as the last ice crystal was melted, the cells were immediately diluted into medium. These tubes have to be centrifuged for 5 min at 1500 rpm to eliminate the toxic agent, DMSO. Finally, the supernatant was removed by decantation and the pellet resuspended in cRPMI.

• Maintenance of tumor cell lines

Tumoral cells are grown and maintained at 37°C with 5% CO_2 into a humified incubator. Cell culture flasks should be examined daily, observing the morphology, the color of the medium and the density of the cells. Normally, because of cell growth, medium is replaced every two or three days. In this period of time is observed a change of color of red-rose to yellow-brown.

• Harvesting of tumor cell lines (standard protocol for adherent cells)

Tumor cells, a type of adherent cells, are harvested when have reached a too much population density or it is interested in carrying out an essay.

Firstly, it was removed and discarded the spent cell culture medium from each culture flask and proceeding with the wash step, without wasting any time to prevent cell drying. To this end, PBS (wash solution) was gently added on the opposite side of the attached cell layer of the vessel to avoid disturbing it, and rock the vessel back and forth several times (repeat twice in total). This wash step removes any traces of serum, calcium, and magnesium, apart of dead cells or other impurities, that they would inhibit the action of the dissociation reagent.

Secondly, it was removed and discarded the wash solution from each culture vessel and was added the pre-warmed accutase (trypsin) into the tumor cells. This is a dissociation reagent to disengage the cells from the vessel. It was used enough reagent to cover the cell layer, gently rocking the container to get complete coverage of the cell layer. It now was incubate the culture vessel at 37º for 3-7 min (the actual incubation time varies with the cell line used) to facilitate cell separation. In difficult cases, it can tap the vessel to expedite cell detachment.

Thirdly, once cells were been detached, it was added the equivalent of twice the volume used for the dissociation reagent of pre-warmed complete growth medium to neutralize the trypsin effect. It was dispersed the medium by pipetting over the cell layer surface several times. Then, tumor cells were transferred to a conical tube and were centrifuged, at 200 × g during a few minutes (about 7 min), for removing pollutants.

Finally, the cell pellet was resuspended in a minimal volume, depending on the estimated cell density, of pre-warmed cRPMI for cell counting.

• Counting of tumor cells

It is essential to know the tumor cell concentration for each sample before carrying out an experiment, to work with the appropriate conditions and obtaining reproducible essay. Therefore, 100 µL of tumor cell sample are removed and mixed 1:1 with 4% trypan blue solution, a diazo dye, which distinguishes between dead and living cells. Viable cells, with intact cell membranes, exclude trypan blue while dead cells stain blue due to trypan blue uptake. Then, the total number of cells is calculated using a hemacytometer. This is a counting chamber which determines the cell concentration in a liquid sample.

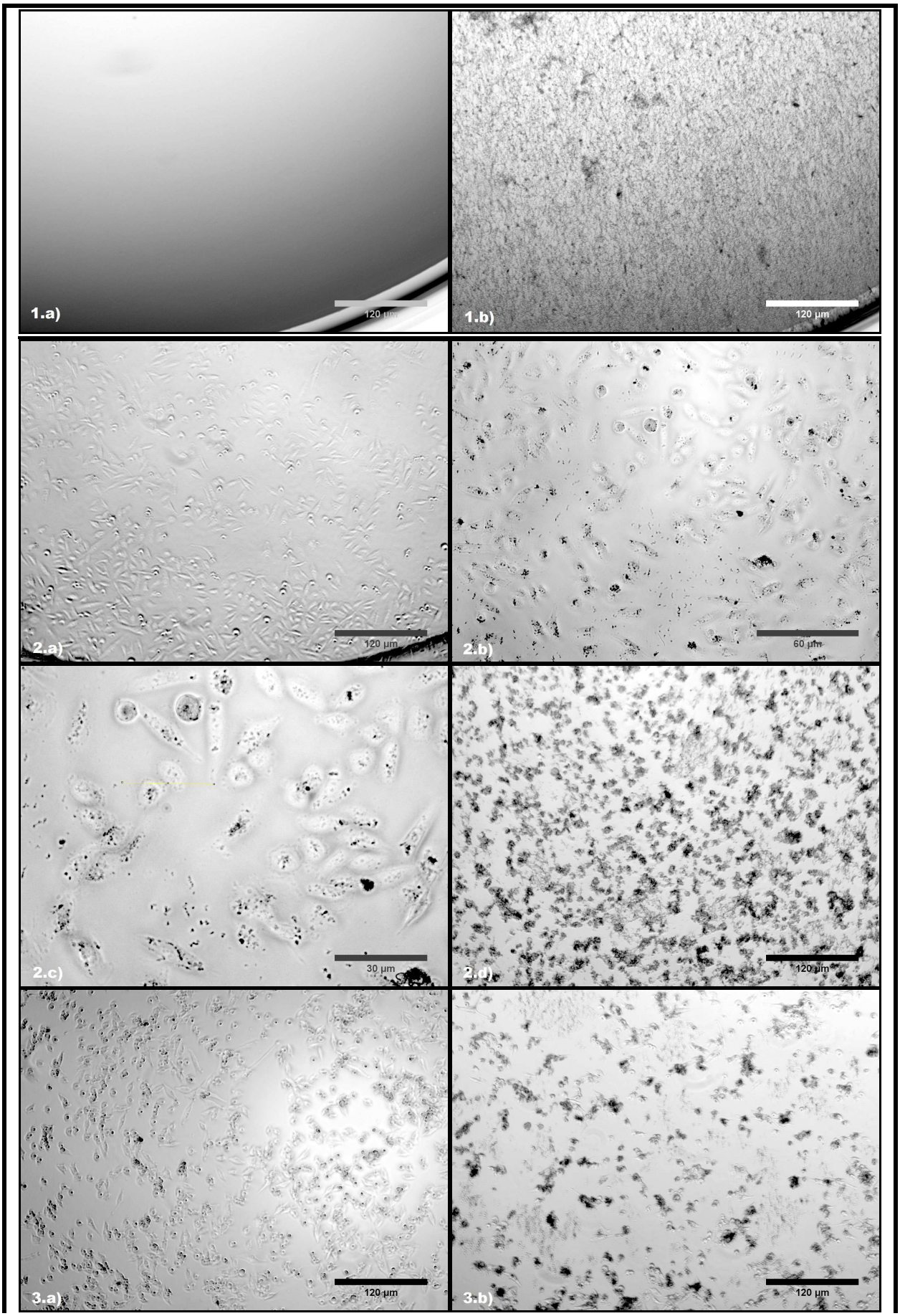
1.a)
120 µm
1.b)
120 µm
2.a)
120 µm
2.b)
60 µm
2.c)
30 µm
2.d)
120 µm
3.a)
120 µm
3.b)
120 µm

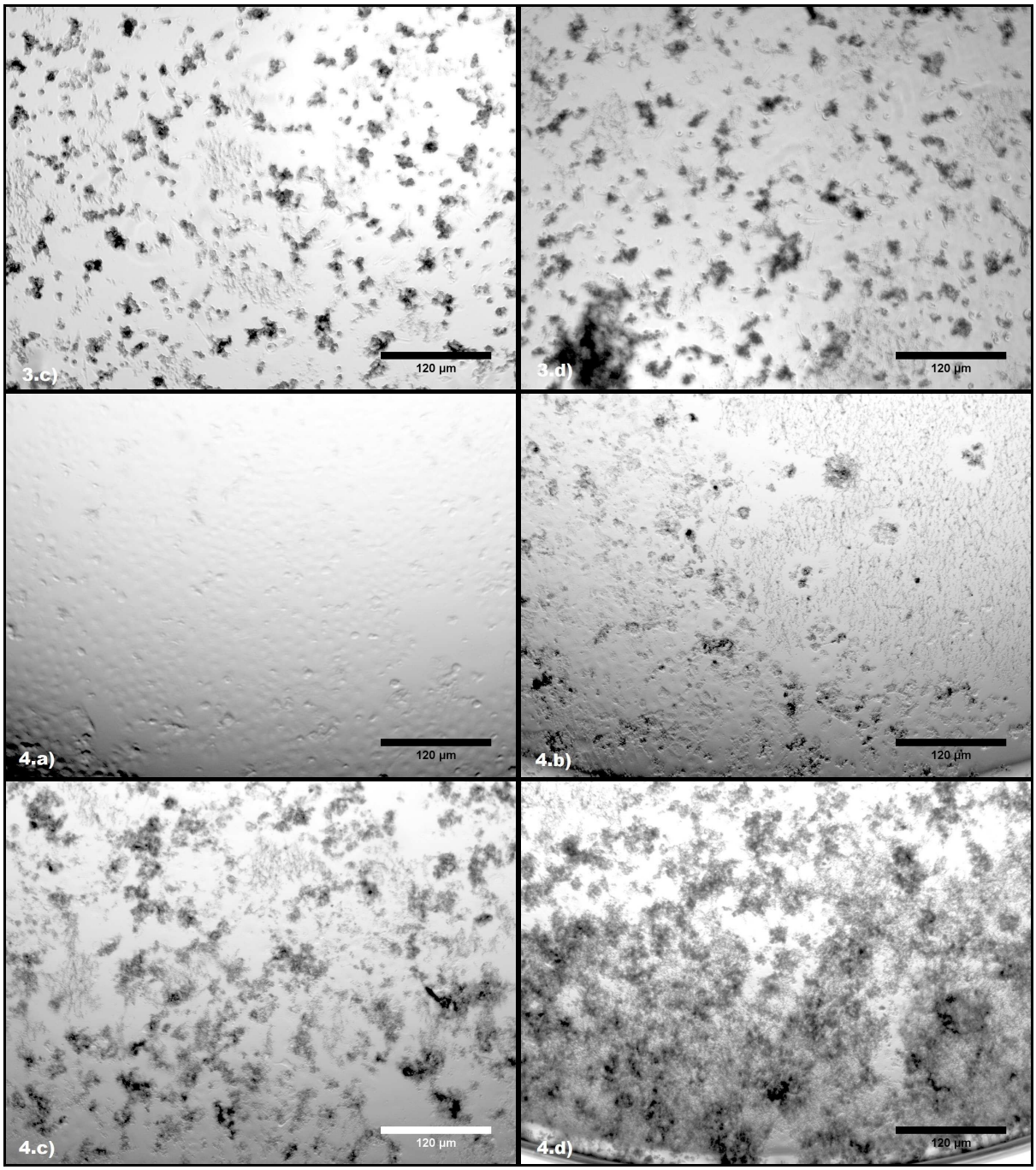

FLUORESCENCE IMAGES OF THE CYTOTOXICITY ESSAYS. **1)** Blank (only MNPs): **1.a)** 0 µg mL^{-1}, **1.b)** 100 µg mL^{-1}. **2)** MNPs_MDA-MB-213_12h: **2.a)** 0 µg mL^{-1}, **2.b)** 5 µg mL^{-1}, **2.c)** 5 µg mL^{-1}, **2.d)** 100 µg mL^{-1}. **3)** MNPs_MIA PaCa-2_36h: **3.a)** 0 µg mL^{-1}, **3.b)** 50 µg mL^{-1}, **3.c)** 100 µg mL^{-1}, **3.d)** 200 µg mL^{-1}. **4)** MNPs_PCI-13_60h: **4.a)** 0 µg mL^{-1}, **4.b)** 50 µg mL^{-1}, **4.c)** 100 µg mL^{-1}, **4.d)** 200 µg mL^{-1}. *Images taken by the inverted fluorescence microscope AXIOVERT 40 CEL in the image service of the Hillman Cancer Center (Pittsburgh, USA).*

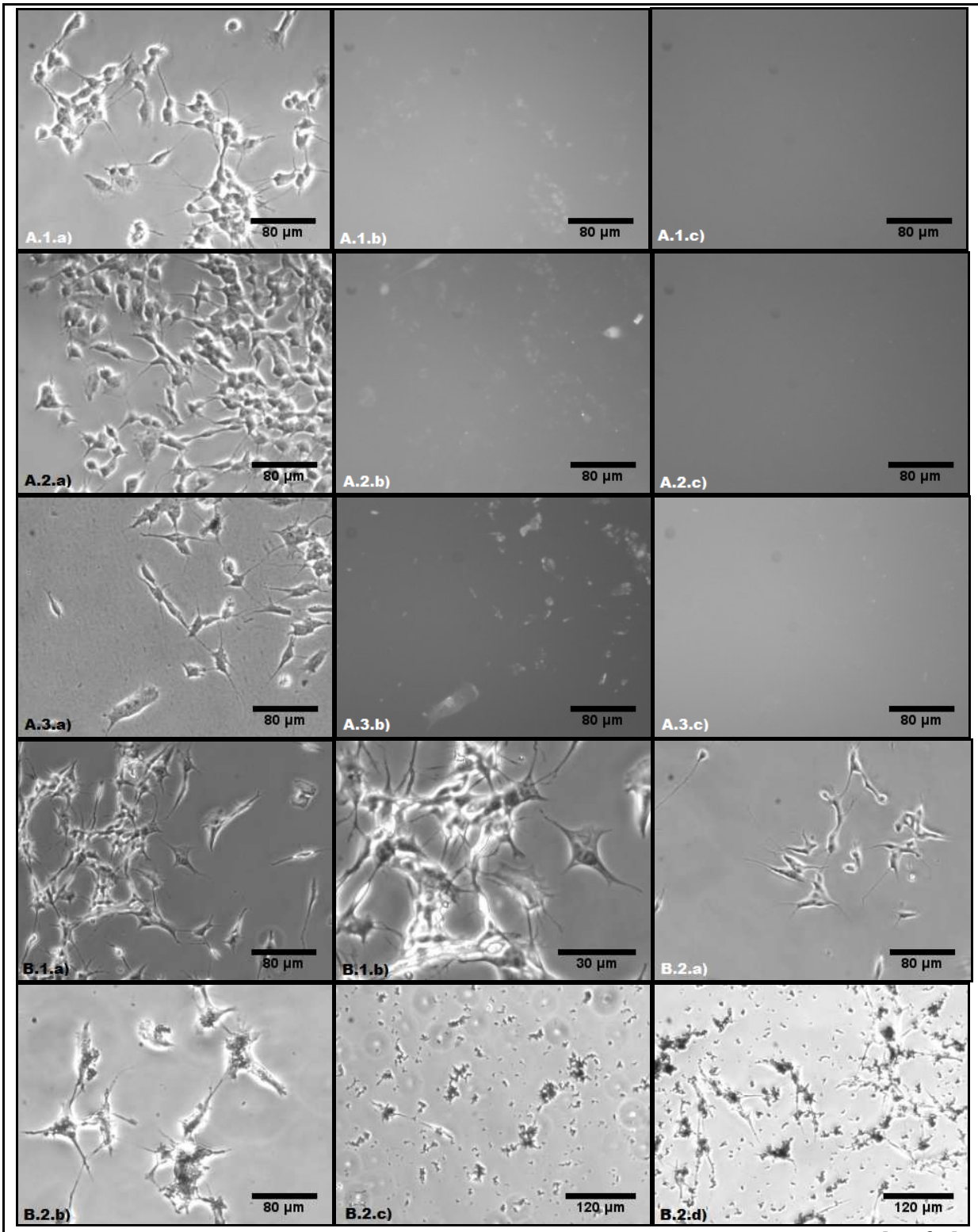

▪ **FLUORESCENCE IMAGES OF THE SH-SY5Y TUMOR CELL LINE**. **A) Study of the interaction between MNPs:anti_CDs in TRIS buffer, pH:7.9**. SUPERNATANTS: cells + 5 µL of each anti CDs + MNPs**. A.1)** 5 µg mL^{-1} MNPs: **A.1.a)** Without filter, **A.1.b)** Green filter, **A.1.c)** Red filter. **A.2)** 25 µg mL^{-1} MNPs: **A.2.a)** Without filter, **A.2.b)** Green filter, **A.2.c)** Red filter. **A.3)** 100 µg mL^{-1} MNPs: A.3.a) Without filter, **A.3.b)** Green filter, A.3.c) Red filter. **B) Preparation samples for SEM**. **B.1)** BLANK1 (only cells)**: B.1.a)** cells, 20X, B.1.b) cells, 40X. **B.2)** BLANK2 (cells + MNPs): **B.2.a)** 1 µg mL^{-1} MNPs, **B.2.b)** 5 µg mL^{-1} MNPs, **B.2.c)** 25 µg mL^{-1} MNPs, **B.2.d)** 100 µg mL^{-1} MNPs. *Images taken by the inverted fluorescence microscope NIKON ECLIPSE TE2000-S in the image service of the INA.*

■ *APPENDIX 2*

▪ *BASIC PROTOCOLS FOR WORKING WITH PHAGES*

• Culture media

- LB-Agar plates: To prepare 5 plates: 100 mL of pre-warmed LB-Agar (5 plates per 100 mL), warming up in the microwave, is poured in every plate, filling 1/3 of the plate, and wait to solidification. Store the plates upside down wrapped with parafilm, to prevent them from drying out, and store at 4ºC.
- IPTG/XGal_LB-agar plates. To prepare 25 plates: 0.1 mM of IPTG and XGal (corresponds to 100 μL/200 μL of 0.1 M IPTG/0.05 M XGal stock solution, respectively) were added into 100 mL of LB-Agar (8 plates per 100 mL), previously dissolved and cooled to 65ºC or less. As quickly as possible after their preparation, the solution is poured into the plates, until cover the surface completely, and wait to solidification. Store the plates upside down inside the bag at 4ºC.

• Culture bacteria

- Preparation of plating bacteria: To prepare 3 E.coli_LB-Agar plates: Streak out the master stock culture of E. coli K12 ER2738 onto each LB-Agar plate, helped by a sterile stick. Then, the plates were inverted and incubated at 37ºC overnight. Store for a maximum of 2 weeks, wrapped with parafilm at 4ºC in the dark.
- Preparation of bacteria solution: To prepare 100 mL of E.coli_LB solution: Firstly, 100 mL of LB were inoculated, in a 100 mL sterile erlenmeyer, with a single well-isolated bacterial colony, picked from the minimal agar plate previously prepared. Then, 133 μL of Tetracycline (7.5 mg mL^{-1}) were added to the solution. Tetracycline is a broad-spectrum polyketide antibiotic (explain). Finally, the liquid culture was agitated, in a rotatory shaker, overnight at 37ºC and 180 rpm.

    ▫ *Note*: It must work in the amplification process with values of OD around 0.5 for the bacteria solution, because this corresponds at the beginning of the exponential phase.

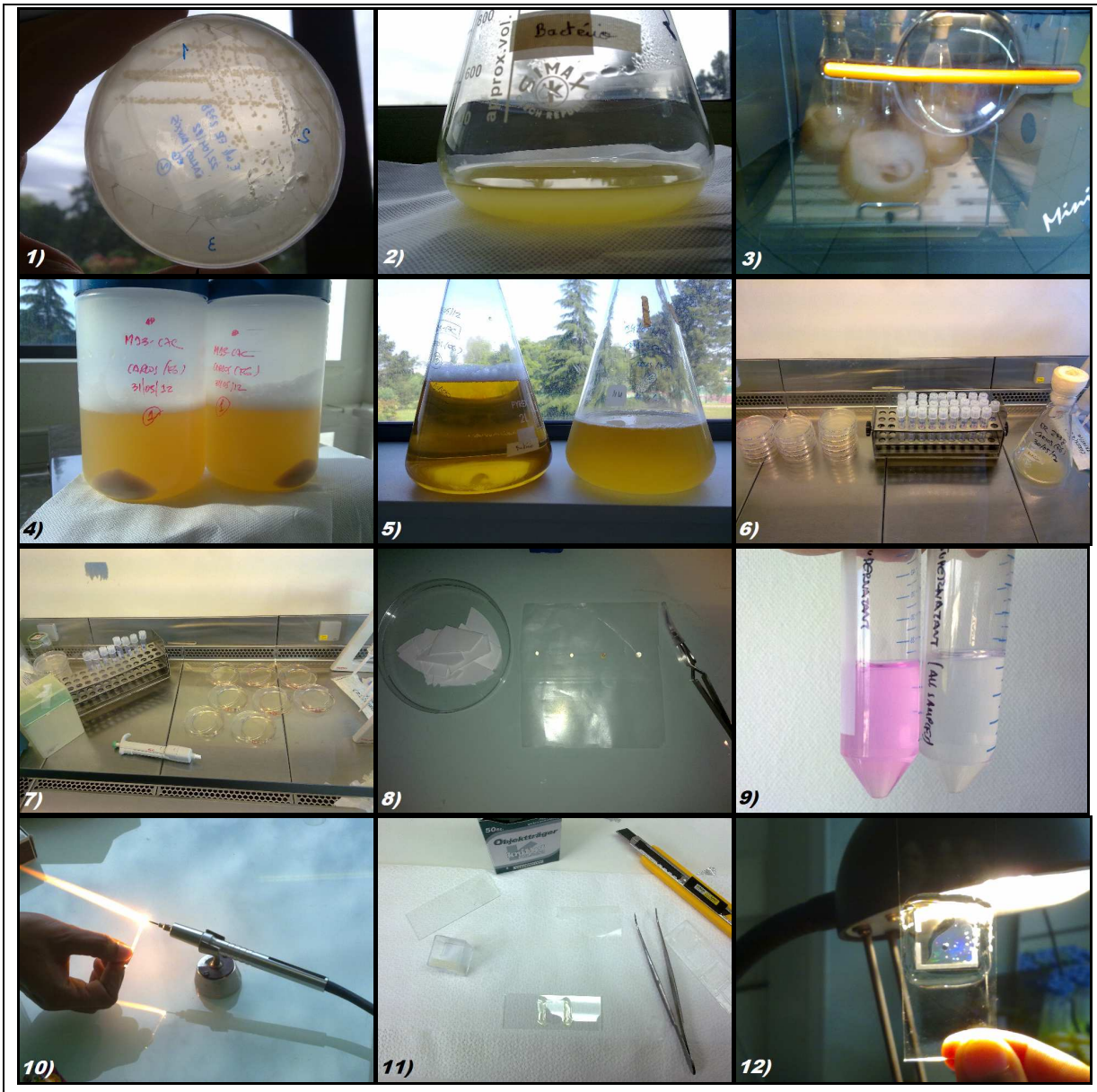

▪ **<u>PHOTOS TAKEN DURING THE COURSE OF THE PROJECT</u>**. **1)** PREPARATION OF PLATING BACTERIA: E.coli K12 ER 2738 grown in LB medium. **2)** PREPARATION OF SOLUTION BACTERIA: Turbid solution after overnight incubation. **3)** AMPLIFICATION PROCESS: Incubation process. **4)** PURIFICATION PROCESS: Step 1_Elimination bacteria-Plastic bottles with the bacteria pellets after the centrifugation process. **5)** PURIFICATION PROCESS: Steps 2-3_Comparation between both samples: after the depletion process (turbid solution) and after the step3-erlemeyer containing the supernatant removed (clear solution). **6)** TITRATION PROCESS: Preparing the phage dilutions. **7)** TITRATION PROCESS: Let cool down the IPTG/XGal-LB agar plates with the top agar-dilutions samples. **8)** SAMPLE PREPARATION FOR SEM: M13-C7C sample and washing solutions. **9)** FLUORESCENCE LABELLING PROCESS: Removing the excess of dye by centrifugation process. **10)** SAMPLE PREPARATION FOR LIQUID CRYSTALS STUDIES: Melting the ends of capillary to seal hermetically. **11)** SAMPLE PREPARATION FOR LIQUID CRYSTALS STUDIES: Sealing the sides of sample with UV polymer glue. **12)** SAMPLE PREPARATION FOR LIQUID CRYSTALS STUDIES: Iridescence phenomena observed within the sample with Sm phase organization. *All Photos were taken at the Centre de Recherche Paul Pascal (CRPP-CNRS), Bordeaux, France.*